

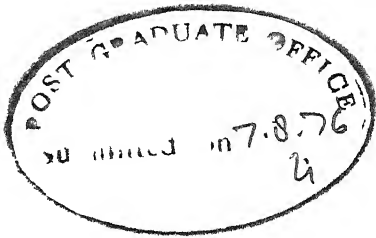
# **ELECTRICAL PROPERTIES OF BOROSODASILICATE GLASSES CONTAINING $Sb_2 O_3$ AND $Bi_2 O_3$**

**A Thesis Submitted  
in Partial Fulfilment of the Requirements  
for the Degree of  
MASTER OF TECHNOLOGY**

**By  
B. V. HIREMATH**

**to the**

**INTERDISCIPLINARY PROGRAMME IN MATERIALS SCIENCE  
INDIAN INSTITUTE OF TECHNOLOGY KANPUR  
AUGUST, 1976**



(i-)

CERTIFICATE

This is to certify that this work on "Electrical Properties of Borosodasilicate Glasses Containing  $Sb_2O_3$  and  $Bi_2O_3$ " by B.V. Hiracheth has been carried out under my supervision and has not been submitted elsewhere for a degree.

D. C. Chakravorty

(D. Chakravorty)

Professor

Department of Metallurgical Engineering  
Indian Institute of Technology, Kanpur

POST GRADUATE OFFICE
This thesis is submitted
for the degree of
of
in accordance with the
regulations of the
Institute of Technology
Dated 12.8.76

MS-1976-M-HIR-ELE

IT  
CENTRAL  
Acc. No. 47068

### ACKNOWLEDGEMENT

I express my heart felt gratitude to Professor D. Chakravorty for his excellent and enthusiastic guidance throughout the course of my research work.

I am thankful to Prof. E.C. Subbarao for his advice and encouragement.

My sincere thanks are due to Mr. Devendra Kumar, Mr. Holliyal Arvind and Mr. H.R. Aravinda for their help in experimental work.

The help rendered by Mr. B. Sharma, Mr. R.D. Prasad and Mr. O.P. Malaviya is gratefully acknowledged.

My thanks are also due to Mr. R.N. Srivastava for his excellent typing and Mr. Vishwanath Singh for his help.

The financial assistance received for the project from Council of Scientific and Industrial Research is gratefully acknowledged.

B.V. Hiremath

CONTENTS

<u>CHAPTER</u>		<u>Page</u>
LIST OF FIGURES		(vii)
SYNOPSIS		(viii)
1. INTRODUCTION		1
1.1 Classification of Amorphous Semiconductors		1
1.2 Characteristics of Amorphous Semiconductors		2
1.3 Electrical Conductivity		3
1.3.1 Ionic Conductivity		3
1.3.2 Temperature Dependence of Ionic Conductivity		4
1.3.3 Ionic Conductivity and Ionic Diffusion		5
1.3.4 Mixed Alkali Effect		5
1.4 Electronic Conduction		6
1.4.1 Theory of Amorphous Semiconductors		6
1.5 Switching Properties		8
1.5.1 Threshold Switching		8
1.5.2 Memory Switching		9
1.6 Ion-exchange and Reduction Treatments		10
1.6.1 Reduction		10
1.6.2 Ion-exchange and Reduction		10
1.7 Studies of Glasses Containing Antimony Oxide and Bismuth Oxide		11

<u>CHAPTER</u>		<u>Page</u>
1.7.1	Microstructural Studies	11
1.7.2	Switching Studies	13
1.7.3	Anamolous Behaviour of $Sb_2O_3$ and $As_2O_3$ Glasses	15
2.	STATEMENT OF THE PROBLEM	16
3.	EXPERIMENTAL PROCEDURE	18
3.1	Glass Preparation	18
3.2	Sample Preparation	19
3.2.1	Bulk Resistivity Measurements	19
3.2.2	Surface Resistivity Measurements	19
3.3	Resistivity Measurements	20
3.3.1	High Temperature Resistivity Measurements	21
3.3.2	Low Temperature Resistivity Measurements	21
3.4	Switching Properties	22
3.5	Optical Absorption Spectra	22
3.6	Differential Thermal Analysis	22
4.	RESULTS	23
4.1	Bulk Resistivity Measurements	23
4.2	Surface Resistivity Measurements	24
4.2.1	Virgin Glasses	24
4.2.2	Reduced Glasses	26
4.3	Switching Studies	28

<u>CHAPTER</u>		Page
4.4	Optical Absorption	28
4.5	Differential Thermal Analysis	29
5.	DISCUSSION	34
5.1	Bulk Resistivity	34
5.2	Surface Resistivity	36
5.2.1	Virgin Glasses	37
5.2.2	Reduced Glasses	38
5.2.3	Ion-exchanged and Reduced Glasses	39
5.2.3.1	Low Temperature Measurements	39
5.2.3.2	High Temperature Measurements	40
5.3	Switching	43
5.4	Optical Absorption	43
5.5	Differential Thermal Analysis	43
6.	CONCLUSION AND SCOPE FOR FURTHER WORK	45
6.1	Conclusions	45
6.2	Scope for Further Studies	46
	REFERENCES	48

LIST OF FIGURES

## FIGURE

- 1 Circuit diagram for resistivity measurements  
2-9 Variation of bulk resistivity with temperature  
10 Variation of activation energy with the ratio of concentration of  $Sb_2O_3$  to  $Bi_2O_3$   
11-12 Variation of surface resistivity of virgin glasses  
13-15 Variation of surface resistivity of reduced glasses  
16-23 Variation of surface resistivity of IER glasses  
24 Switching characteristics of IER glasses  
25 Absorptical absorption curves for virgin glasses  
26 DTA curves for virgin glasses.

SYNOPSIS

An investigation of electrical, switching and optical properties of various glasses containing both  $Sb_2O_3$  and  $Bi_2O_3$  in  $Na_2O-B_2O_3-SiO_2$  glass matrix was carried out.

The variations of bulk conductivity of these glasses and surface conductivity of virgin glasses,  $Na^+ \leftrightarrow Ag^+$  ion-exchanged and reduced and simply reduced glasses in hydrogen were studied as a function of temperature.

The rigidity of the borosilicate glass matrix is found to depend on the ratio of concentration of  $Sb_2O_3$  to  $Bi_2O_3$ . The d.c. conductivity in the bulk glasses in the temperature range 50–400°C is believed to arise from movement of alkali ions. The surface resistivities of virgin glasses are higher than those of ion-exchanged and reduced or simply reduced glasses. Ionic conduction and electronic conduction are believed to be effective in determining the surface conductivities. At low temperatures the electronic hopping between two conducting islands is believed to give low activation energy for ion-exchanged and reduced glasses.

Some of ion-exchanged and reduced glasses were found to exhibit "memory" type of switching.

## CHAPTER 1

### INTRODUCTION

In recent years there has been a tremendous revival of research activities in amorphous materials mainly due to the projected technological importance of these materials. Because of ease of fabrication of amorphous switches in planar or sandwiched structure and the possibility of direct incorporation into integrated circuits, these materials are considered to have tremendous application potential<sup>(1)</sup>. The wide spectrum of applications of these materials includes switching and memory devices, continuous dynode electron multipliers, optical mass memories, high energy particle detectors, phase contrast holograms, infrared lenses, ultrasonic delay lines and microfiche transparencies.

#### 1.1 Classification of Amorphous Semiconductors

The examples for various kinds of amorphous semiconductors are, elemental such as S and Se<sup>(2)</sup> and compounds like vanadate-phosphate<sup>(3,4)</sup>, vanadate-germanate<sup>(5)</sup>, Ge-Tc<sup>(6)</sup>, As<sub>2</sub>Tc.Tl<sub>2</sub>Se<sub>3</sub><sup>(7)</sup>, As<sub>2</sub>Tc<sub>3</sub><sup>(8)</sup>, 4As<sub>2</sub>Se<sub>3</sub>.2Sb<sub>2</sub>Se<sub>3</sub><sup>(9)</sup>, As<sub>2</sub>S<sub>3</sub><sup>(10)</sup>, V<sub>2</sub>O<sub>5</sub>-GeO<sub>2</sub>-BaO<sup>(11)</sup>, TiO<sub>2</sub>-B<sub>2</sub>O<sub>3</sub>-BaO<sup>(12)</sup> etc.

These glasses can be broadly classified according to their structural and chemical composition, into 3 categories viz., (1) elemental, (2) covalent alloys and (3) ionic or tightly bound.

The first category contains elements, of which only S and Se can be obtained in amorphous form by slow cooling of their melts. Because of their chain or ring structure, the short range order extends over rather long distances depending on temperature and thermal history of the material. The second category contains alloys of group IV, V and VI. These possess compositional as well as translational disorder. The materials belonging to the third category have positional disorder and impurities as an additional type of disorder. These materials have band gaps larger than 2 eV.

## 1.2 Characteristics of Amorphous Semiconductors

Several phenomena in amorphous semiconductors can be observed with sufficient frequency to regard them as characteristic of amorphous phase and they are:

1. Electrical or thermal energy gaps of approximately the same magnitude as those occurring in the crystalline phase (where this exists)<sup>(13-15)</sup>.

2. Coexistence of two basic conduction mechanisms, band conduction and hopping between localized states<sup>(16)</sup>.
3. Conductivities which increase with frequency of the applied field<sup>(17)</sup>.
4. Non-ohmic behaviour at high fields<sup>(18,19)</sup> (followed by switching in some materials).
5. Temperature activated drift mobilities<sup>(20,21)</sup>.
6. Anomalous Hall effect<sup>(22)</sup>.
7. Electrical field dependent quantum efficiency<sup>(23,2)</sup>.
8. Exponential optical absorption edges<sup>(23)</sup>.
9. Optical energy gap greater than electronic energy gap<sup>(24,25)</sup>.
10. Relaxation of the k-conservation selection rule for optical transitions<sup>(26)</sup>.

### 1.3 Electrical Conductivity

Conduction in glasses can be either ionic or electronic in nature depending upon the nature of glass and the temperature range.

#### 1.3.1 Ionic conductivity

The basic ingredients of oxide glasses are a "network former" e.g.,  $\text{SiO}_2$ , "modifier" e.g.,  $\text{Na}_2\text{O}$ ,  $\text{CaO}$

and an "intermediate" e.g.,  $\text{Al}_2\text{O}_3$ . These modifiers are electrostatically attached to the "non-bridging" oxygen ions and they are considered to be the principal carriers.

Oxide glasses containing large amounts of alkali ions are essentially electrolytic conductors as shown by Littleton et al.<sup>(27)</sup>. The ionic conductivity of many oxide glasses results from the transport of monovalent cations, and usually the mobility of divalent ions is low relative to alkali ions.

### 1.3.2 Temperature dependence of ionic conductivity

The electrical resistivity  $\rho$  of most of the oxide glasses is generally described by Rasch-Hinrichsen<sup>(28)</sup> relation

$$\log \rho = A + B/T \quad (1.1)$$

where A and B are constants.

The theoretical model used by Frenkel<sup>(29)</sup> for ionic transport in crystalline solids is generally adopted for glasses, in which an alkali ion will move from one potential well to another, preferentially in the direction of applied field.

Various models to explain the relationship between conductivity, temperature and the nature of the

glass network have been proposed by Stevens<sup>(30)</sup> and Mazurin<sup>(31)</sup>.

### 1.3.3 Ionic conductivity and ionic diffusion

From the theoretical considerations on the random jump of ions as the rudimentary step leading to ionic behaviour, it is obvious that ionic conductivity is closely related to ionic diffusion<sup>(32)</sup>. The electrical conductivity of glass is related to the diffusion coefficient of the ion by Nernst-Einstein relation<sup>(33)</sup>

$$\sigma = \frac{Z^2 F^2 D C}{RT} \quad (1.2)$$

where D is the ionic diffusion coefficient in  $\text{cm}^2/\text{sec}$ , F is the Faraday constant, R is the gas constant in Joules/mole-deg., C is the concentration of ions in moles/ $\text{cm}^3$  and Z is the ionic valence. Equation (1.2) is useful in assessing conduction mechanisms in glasses and it has been found that calculated data are in confirmation with the experimental data<sup>(32,33)</sup>.

### 1.3.4 The mixed alkali effect

When a second alkali is added to an alkali silicate glass the conductivity decreases sharply<sup>(34)</sup>. The

mixed alkali effect has been reported for a wide variety of oxide glasses besides silicate glasses like borates, germanates etc. However, for any significant effect, the alkali concentration should exceed 10%<sup>(35)</sup>. Many theoretical models have been proposed to explain the mixed alkali effect.

It has been also found that ionic conductivity of oxide glasses depends on the composition of the glass<sup>(36)</sup>, applied pressure<sup>(37)</sup> and thermal history of the glasses<sup>(38)</sup>.

#### 1.4 Electronic Conduction

In most of the amorphous semiconductors conduction is considered to take place by hopping of carriers from one strongly localised state to another. For example, glasses containing transition element such as Fe in  $V_2O_5-P_2O_5$ , hopping of carriers will take place from one valence (localised) state to another of transition metal. The conductivities of these glasses vary according to the relation  $\sigma = \sigma_0 \exp(-E/kT)$  where  $\sigma_0$  is constant and E is activation energy.

##### 1.4.1 Theory of amorphous semiconductors

Several theories have been proposed to explain the electronic conduction in these materials which will be discussed in the next section.

Most of the theoretical approaches have started with standard band theory of crystalline solids and have assumed perturbations to this model, the perturbation taking the form of annihilating the long range order, over a few atomic spacings whilst maintaining the short range order.

In Cohen-Fritzsche-Ovshinsky<sup>(39)</sup> model, each localised imperfection is considered to be a 'localised' state in the gap between two bands, due to variation in potential energy. A carrier in the localised states moves by Phonon-assisted hopping and its mobility is therefore less by 2 or 3 orders to that of in "extended" states where the carriers are subjected to many scattering process, Hence there exists a "mobility gap" which replaces the density states gap in case of crystalline semiconductors.

Mott<sup>(40-42)</sup> has used theory of Anderson<sup>(43)</sup> to account for the existence of localised states. He has shown that there is a discontinuous change in conductivity at the band edges. Gubanov<sup>(44)</sup> considered the glassy model as a "frozen" liquid in which potential wells of random depth are assumed to give rise to localised states.

It is to be noted that all the models predict "tail" states extending to several tenths of an eV and localised states densities of  $10^{18}$ - $10^{19} \text{ cm}^{-3}$ . We notice that these models differ in their origin for the cause of

the localised states. Cohen finds they arise from density fluctuations in a random atomic structure; Mott—from random well depths in a periodic well structure; and Gubanov—from random spacings of wells of uniform depth with a small effect due to well depth variations. All these models have been recently reviewed by Hulls et al.<sup>(45)</sup>.

### 1.5 Switching Properties

One of the most interesting properties of glasses is the phenomenon of electronic switching. There are two types of switching<sup>(46)</sup>; threshold switching and memory switching.

#### 1.5.1 Threshold switching

As the applied voltage of the sample is increased, at a critical voltage called "threshold" voltage, the material switches from high resistance ("OFF") state to low resistance ("ON") state and below a certain holding current through it, the material switches back to OFF state. This is reversible. The threshold voltage is found to depend on temperature as well as separation between the electrodes.

Many mechanisms have been put forward to describe the threshold switching and they are:

- (i) Electronic mechanism<sup>(47,48)</sup>
- (ii) Phase change mechanism<sup>(49,50)</sup>
- (iii) Purely thermal breakdown<sup>(51,52)</sup>.

However, no theory is complete in accounting for all the switching of the glasses.

#### 1.5.2 Memory switching

As we increase the voltage across the material it switches to "ON" state. The conductive "ON" state will be maintained even after the switching voltage is removed. In other words an irreversible transformation from an insulating state to a conductive state has occurred. Through proper pulsing the material can be made to return to "OFF" state. The memory effect has generally been associated with a glass-to-crystal transition. Conductivity could be due to the formation of filaments embedded in the glass and bridging the electrodes. While pulsing the remelting of the filaments occurs which results in high conductive "OFF" state.

Whether a glass will show "threshold" or "memory" behaviour is dependent on its chemical composition. For instance, a glass with composition 10Ge - 30As - 12.6Si - 47.7Te (atomic %) shows threshold switching whereas another

one with composition 10Ge - 50As - 40Te (atomic %) shows memory behaviour<sup>(52)</sup>.

### 1.6 Ion-Exchange and Reduction Treatments

#### 1.6.1 Reduction

It is found that resistivities of certain oxide glasses will decrease if the surface is given reduction treatment by hydrogen. Green and Blodgett<sup>(53)</sup> have studied the electrical properties of  $\text{Bi}_2\text{O}_3$  and PbO glasses after subjecting to reduction treatment by hydrogen. They have found that the surface conductivity of the reduced glasses was as low as 100-1000 ohm/square. The surface conductivities of the reduced glasses were found to depend on the distance between the particles, influence of surrounding oxide lattices and composition of the glasses<sup>(54)</sup>.

#### 1.6.2 Ion-exchange and reduction

When a glass is immersed in molten bath like  $\text{AgNO}_3$ , or  $\text{CuCl}$  or  $\text{CuCl}_2$ , at the glass-salt interface ions move in and out of the glass governed by ion-exchange mechanism. If the ion-exchange treatment is carried out above the glass transition temperature  $T_g$ , the network of glass adjusts itself to the differing partial molar volumes

of the exchange ions. When the temperature is less than  $T_g$  it results in a stress in the glass. If the salt bath ions are larger than the host ions in the glass there is a resultant compression which increases the strength of the glass (55).

### 1.7 Studies of Glasses Containing Antimony Oxide and Bismuth Oxide

Several glasses containing  $B_2O_3-Bi_2O_3$ ,  $B_2O_3-Sb_2O_3$ ,  $CaO-Bi_2O_3$ ,  $Al_2O_3-Bi_2O_3$ ,  $PbO-B_2O_3$  in  $Na_2O-SiO_2$  base glass matrix and "float" glass containing  $SiO_2-Na_2O-CaO-MgO-K_2O-SO_3-Al_2O_3-Fe_2O_3$  have been extensively studied by Chakravorty et.al. (56,57) The former group glasses was treated with sodium  $\rightleftharpoons$  silver ion exchange followed by reduction in hydrogen whereas the latter group was treated with sodium  $\rightleftharpoons$  copper ion exchange and ion reduction in hydrogen.

#### 1.7.1 Microstructural studies

It has been found that the microstructural features of all the glasses containing  $Bi_2O_3$  were similar. The electron micrographs of the surface of the virgin glass reveals that it consists of a dispersion of spherical particles of metallic bismuth with diameters ranging from 50-800 Å, embedded in glassy matrix. After ion exchange and subsequent reduction larger particles with maximum

diameter of about 2000  $\text{\AA}^{\circ}$  metallic silver are found to appear in the glass matrix.

However, the droplet phase in virgin specimen of  $\text{Sb}_2\text{O}_3$  containing glass is found to be rich in antimony but not in metallic state. The ion exchanged and reduced specimen has a structure consisting of fine silver droplets of diameters measuring from 50-100  $\text{\AA}^{\circ}$ .

In case of  $\text{Al}_2\text{O}_3$  containing glasses the droplet phase in virgin sample is rich in bismuth which however is not in metallic state. After ion exchange and reduction the droplets become much smaller ranging from 50-150  $\text{\AA}^{\circ}$  and after reduction metallic silver droplets appear having diameters measuring from 50-650  $\text{\AA}^{\circ}$ .

It is to be noted that in all the cases metallic silver particles with diameters measuring from 50-2000  $\text{\AA}^{\circ}$  are found to appear in dispersed glass matrix.

The electron micrograph of the surface of "float" (57) glass shows no phase separation before ion exchange and reduction treatment. After (copper-sodium) ion exchange done at high temperature ( $650^{\circ}\text{C}$ ) the sample shows phase separation due to injection of copper ions into glass.

### 1.7.2 Switching studies

Memory switching has been observed by Chakravorty<sup>(58)</sup> and Devendra Kumar<sup>(59)</sup> in surface layers containing  $\text{Bi}_2\text{O}_3$  and  $\text{Sb}_2\text{O}_3$  separately in  $\text{Na}_2\text{O}-\text{B}_2\text{O}_3-\text{SiO}_2$  base glass matrix. Chakravorty and Murthy<sup>(60)</sup> have observed negative resistance and memory switching in thin films of  $\text{Na}_2\text{O}-\text{Bi}_2\text{O}_3-\text{B}_2\text{O}_3-\text{SiO}_2$  glasses.

The switching observed in bismuth glasses has been ascribed to its microstructural characteristics. The sample switches to the "ON" state upon application of an electric field which presumably induces crystallisation of the glass phase between the metallic bismuth "islands". A high current pulse of short duration melts these crystals which are then quenched back to the glassy phase to give "OFF" state.

It is to be noted that the surface roughness of the glasses is necessary for obtaining the high conductance effect. It is believed that imperfections introduced in the surface by grinding operation increase the efficiency of metallic particles which can then grow sufficiently to form a continuous chain.

Chakravorty et.al.<sup>(60)</sup> have attributed the possibility for the "OFF" state conduction to the electron

hopping between conducting islands of bismuth in case of thin films of bismuth glasses. The activation energy for electron hopping in such a situation has been shown by Neugebauer and Webb<sup>(64)</sup> to be given by  $e^2/Kr$  where e is the electronic charge, K is the dielectric constant of the glassy matrix, and r is the diameter of the conducting island. Assuming a value of K = 6 (Chakravorty et.al.<sup>(61)</sup>) one calculates from the spread of activation energies mentioned above a range of r values extending from 10-150 Å. This is consistent with the microstructural features of these glasses as we have seen in earlier section.

The negative resistance obtained in these glass films is considered to arise from a Joule-microheating process<sup>(62)</sup>. It has been found by extrapolation of the plot of threshold voltage versus temperature for the glass films, that at about 450°C, the glass film would switch without application of electric field and switch off temperature was found close to melting point of bismuth metal. These glasses tend to crystallize in the temperature range 500-600°C, the crystalline phase having a lower resistance than the parent glass<sup>(61)</sup>.

Thus they conclude that if the "ON" state is assumed to be a result of the formation of bismuth filaments between conducting islands, the switch "OFF" process can

be explained on the basis of a rupture of the filaments.

### 1.7.3 Anomalous behaviour of $Sb_2O_3$ and $As_2O_3$ glasses

Oxide glasses containing  $Sb_2O_3$  in  $Na_2O-B_2O_3-SiO_2$  glass matrix have shown very interesting properties. The resistivities of the ion exchanged and reduced surface of the glasses have been shown by Devendra Kumar<sup>(59)</sup> to have a marked dip at around room temperature.

Similar behaviour has been found by Halliyal Arvind<sup>(63)</sup> in glasses containing  $As_2O_3$  in  $Na_2O-B_2O_3-SiO_2$  glass matrix. He has observed that the surface resistivities of all the virgin, reduced and ion exchanged and reduced glasses exhibit a minimum near room temperature. The resistivities increase both below room temperature and just above room temperature. The increase in resistivity below room temperature is tentatively attributed to proton conduction and the increase just above room temperature is described as due to water molecules and their interaction with silicate network of the glass.

Since alkali borosilicate glasses containing  $Sb_2O_3$  and  $Bi_2O_3$  respectively have shown memory switching behaviour after ion exchange and reduction, it was thought that it would be interesting to study the conduction mechanisms and switching properties, when both  $Bi_2O_3$  and  $Sb_2O_3$  are incorporated in the same  $Na_2O-B_2O_3-SiO_2$  glass matrix.

CHAPTER 2STATEMENT OF THE PROBLEM

Electrical properties of glasses containing  $Sb_2O_3$  and  $Bi_2O_3$  separately in  $Na_2O-B_2O_3-SiO_2$  glass matrix have been studied earlier, and it has been found that these glasses show memory type of switching after ( $Na^+ \rightleftharpoons Ag^+$ ) ion-exchange and reduction treatment. It was thought it would be interesting to study the conduction mechanisms and switching properties when both  $Bi_2O_3$  and  $Sb_2O_3$  incorporated in the same  $Na_2O-B_2O_3-SiO_2$  glass matrix.

The objectives of the present investigation were to study the following:

- (a) Bulk properties: Variation of bulk resistivity of glasses with temperature.
- (b) Surface properties: Variation of surface resistivities of virgin, reduced and ion-exchanged and reduced glasses with temperature.
- (c) Switching properties: To study the switching properties of ion-exchanged and reduced glasses at room temperature and below room temperature.
- (d) Optical properties: To study the absorption spectra of virgin glasses in the visible range.

- (e) Differential thermal analysis.
- (f) To study the above effects as a function of the ratio of concentration of  $Sb_2O_3$  to  $Bi_2O_3$  present in the borosilicate glass system.

## CHAPTER 3

### EXPERIMENTAL PROCEDURE

#### 3.1 Glass Preparation

The glasses containing varying amounts of  $Sb_2O_3$  and  $Bi_2O_3$  were prepared from reagent grade chemicals. The compositions are listed in Table 1.  $Na_2O$  was introduced as carbonate,  $B_2O_3$  as boric acid and rest of the ingredients as oxides. The calculated amounts of the starting materials were mixed with acetone and dried. The dried mixture was taken in a high density alumina crucible and heated electrically in a furnace fitted with globar rods. Temperatures of melting of these glasses were in the range of 1300-1450°C. The melt was poured without keeping for a long time in the molten state into aluminium molds of dimensions about 5 cm x 1 cm x 0.5 cm. Since it was observed that  $Bi_2O_3$  oozes out through the tiny pores of the crucible at high temperature the batch was not kept in molten state for a long time. The glasses were annealed at about 400°C and were furnace cooled over night.

The glasses containing less mole % of  $Na_2O$  like glasses 11-23 were difficult to melt and hence it was necessary to keep the melt at high temperature for a longer time for homogenization.

### 3.2 Sample Preparation

#### 3.2.1 Bulk resistivity measurements

The glass plates of dimensions approximately 2 cm x 1 cm x 1 cm were polished to a thickness of 0.5-1 mm using silicon carbide grit of different mesh sizes (120, 240, 400, 600 and 800 respectively). The silver electrodes were painted uniformly using silver paste (supplied by NPL, India) on both the surfaces and copper wires were affixed to the electrodes. After the paint dried, the specimens were sandwiched between two glass plates (microscope slides) for mechanical support. A guard ring configuration was used to measure the bulk resistivities of the samples.

#### 3.2.2 Surface resistivity measurements

Glass pieces of dimensions approximately 2.0 cm x 1 cm x 0.25 cm were polished using silicon carbide mesh no. 120 for surface resistivity measurements.

For ion-exchange and reduction, these polished glasses were immersed in molten  $\text{AgNO}_3$  bath kept in pyrex crucibles which were heated at 320°C for 6 hours. They were washed in running water to remove any silver nitrate adhering to the surfaces of glasses and then they were given reduction treatment in hydrogen as follows.

The ion-exchanged samples were kept in a furnace and hydrogen gas was passed at a rate of 100 c.c. per minute and the temperature was raised slowly to 320°C. The reduction treatment was carried out for 12 hours. Then these were furnace cooled. Parallel silver electrodes were painted on the surface and copper wires affixed to them as described above. A schematic diagram of the electrode configuration is shown in Fig. 11. Araldite was put on copper leads for mechanical support.

Only reduction treatment was given after polishing another set of samples and electrode leads were fixed as described earlier.

To the virgin glass samples also the electrode leads were put after polishing the sample.

### 3.3 Resistivity Measurements

Bulk resistivity and virgin glass surface resistivity for all the glasses were measured from room temperature to about 400°C, whereas the reduced and ion-exchanged and reduced surface resistivities were measured from room temperature to 320°C, since ion-exchange and reduction treatments were carried out at 320°C. This was to avoid any effect of heat treatment given to the sample by going beyond the temperature at which ion-exchange and reduction treatments were carried out.

### 3.3.1 High temperature resistivity measurements

The circuit used to measure resistivities is as shown in Fig. 1. The sample was put in a horizontal furnace fitted with Aplab temperature controller. The sample was surrounded by metallic tube and the tube was earthed for better shielding purpose. The temperature was increased in steps of 15-25°C and at each constant temperature. (the temperature could be kept constant to within  $\pm 2^\circ\text{C}$ ) the V-I characteristics of the samples were measured either using voltage measuring device like G.R. Electrometer (type 1230-A) or current measuring device like ECIL Digital Picoammeter (type EA813A).

### 3.3.2 Low temperature resistivity measurement

For low temperature resistivity measurement, a set-up given in reference<sup>(59)</sup> was used. The same circuit as used in the high temperature was used to obtain the V-I characteristics. ECIL Electrometer (type EA814) was used as the voltage measuring device.

The V-I characteristics were then fitted to straight line by a least square method using a computer program. The resistivities were calculated by computing slope of these lines.

### 3.4 Switching Properties

Switching characteristics of ion-exchanged and reduced samples were obtained using the same circuit as in the case of high temperature resistivity measurements. For "ON" state characteristic a high resistance ( $10^5$  ohms) was connected in series to sample, to control the current through the circuit.

### 3.5 Optical Absorption Spectra

The virgin glass samples were polished to a thickness of about 0.5 mm using silicon carbide grit of different mesh sizes. Absorption spectra of these samples were recorded using Cary-14 spectrometer in wavelength range 2000-6000 Å. Since ion-exchanged and reduced samples were black, the absorption spectra for these samples could not be obtained.

### 3.6 Differential Thermal Analysis

DTA was carried out taking fine powdered samples of few glasses using "Mon Derivetograph" in the temperature range room temperature to 1000°C by increasing the temperature at a rate of 10°C/min. Pt-Pt/Rh thermocouple and  $\text{Al}_2\text{O}_3$  reference material were used in the investigation.

CHAPTER 4RESULTS

The variation of resistivity with temperature is described by the equation

$$\sigma = \sigma_0 \exp(E/kT) \quad (4.1)$$

where E is activation energy,  $\sigma_0$  is a constant and k is Boltzmann constant. If to the first approximation plots of  $\log \sigma$  vs  $1/T$  are straight lines, the activation energy E and the constant  $\sigma_0$  in the equation (4.1) can be calculated using the standard least squares method of fitting the data.

#### 4.1 Bulk Resistivity Measurements

The variation of bulk resistivities of different glasses in the temperature range 30-400°C are given in figures 2 to 9. The activation energy calculated in different regions of the plots are given in Table 2.

The bulk resistivities of glasses 1, 2, 3, 4, and 5 show similar variation of resistivity with temperature. In the temperature range 20-150°C, the activation energies vary from 0.3 eV to 0.9 eV. In the temperature range 200-310°C activation energies vary from 0.1 to 0.5 eV.

In most of the glasses cooling cycle curves become linear and they differ from heating cycle curves. The bulk resistivities of glasses 12, 21 and 23 are higher than that of glasses 1, 2, 3, 4 and 5. In the case of glass 3, during cooling from 400°C, it switched from a high resistance state ( $10^7$  ohm-cm) to low resistance state ( $10^5$  ohm-cm). This low resistance was quenched using liquid nitrogen, "ON" state characteristics were obtained.

The variation of activation energy calculated in temperature ranges 20-150°C and 200-310°C, with ratio of concentration of  $Sb_2O_3$  to  $Bi_2O_3$  is shown in Fig. 10. We observe that in the former temperature range the activation energy shows a maximum value when the ratio  $Sb_2O_3/Bi_2O_3$  is about one. Whereas in the latter temperature range the activation energy decreases when the ratio  $Sb_2O_3/Bi_2O_3$  increases.

#### 4.2 Surface Resistivity Measurements

##### 4.2.1 Virgin glasses

The surface resistivities of virgin glasses with no surface treatments (ion-exchange or reduction) were measured from room temperature to 400°C. The surface resistivity in ohm/square was calculated using the relation

$$\gamma = \frac{RA}{B}$$

where R is the resistance of the sample in ohms, A is width of electrode and B is the gap of electrode. Geometry of electrodes is shown in Fig. 11.

The variation of  $\log \gamma$  (ohm/ $\omega$ ) with inverse of absolute temperature for virgin glasses 1, 3, 4 and 5 is linear as shown in Fig. 11. For all the glasses the surface resistivities during heating cycle and cooling cycle are approximately the same. Activation energies for the glasses are of the order of 1.0 eV. Virgin glasses 11, 12 and 13 show a hump in  $\log \gamma$  (ohm/ $\omega$ )  $\frac{\text{vs}}{1/T}$  plot at about 120°C as shown in Fig. 12. The values of surface resistivities for all these glasses are of the order of  $10^{14}$  ohm/ $\omega$ . The energies for the glasses above 120°C are of the order of 1.0 eV whereas for temperatures below 120°C, they are of the order of 0.5 eV. It is to be noted that, for the temperatures above 120°C the activation energies for all the glasses are of the same order irrespective of the ratio of concentration of  $Sb_2O_3$  to  $Bi_2O_3$ . The cooling cycle curve show similar behaviour but the orders of magnitude of the resistivities during cooling cycle are smaller than heating cycle.

#### 4.2.2 Reduced glasses

Some of the glasses were only reduced in a current of hydrogen gas without ion-exchange treatment for 12 hours at 320°C. The surface resistivities of the reduced glasses were measured in the temperature range 30° to 320°C. Activation energies of different regions of the plot of  $\log \sigma$  vs.  $1/T$  are tabulated in Table 2.

The variation of resistivity with temperature of reduced glasses 2 and 3 are shown in Fig. 13. It is observed that the plots are linear in the above temperature range. In case of glass 2, cooling cycle curve agrees with heating cycle curve. For glass 3, even though the cooling cycle values of resistivity are slightly higher than that of heating cycle, the variation is similar in both the cycles. Glasses 11 and 12 also show linear behaviour in the temperature range 30-250°C and activation energies are of the order of 0.2 eV. The cooling curves for the glasses differ slightly from heating curves. The plots of  $\log \sigma$  vs.  $1/T$  of glass 13 is shown in Fig. 15. Between 50 to 150°C the surface resistivity of the glass was too high to be measured. Cooling curve also shows similar behaviour even though the resistivities of cooling cycle are lower than that of heating cycle. However, it is to be noted

that the orders of magnitude of resistivity are lower than that of virgin glasses.

#### 4.2.3 Ion-exchanged and reduced (IER) glasses

All glasses were given first ( $\text{Na}^+ \rightleftharpoons \text{Ag}^+$ ) ion-exchange treatment at  $320^\circ\text{C}$  for 6 hours in molten  $\text{AgNO}_3$  bath and then reduced in hydrogen atmosphere at  $320^\circ\text{C}$  for 12 hours. The surface resistivities were calculated from measured resistances of the samples at different temperatures, as described earlier. The resistances of the sample were measured in the temperature range -100 to  $320^\circ\text{C}$ . The plots of  $\log \sigma$  (ohm $^{-1}$ ) vs  $1/T$  are shown in Figures 16 to 23! In the case of IER glasses 3, 4, 5 and 21 minima are observed in the plots of  $\log \sigma$  vs  $1/T$ . It is seen that as the ratio of the concentration of  $\text{Sb}_2\text{O}_3$  to  $\text{Bi}_2\text{O}_3$  increases, (from 1 to 5) the minima move (from room temperature to  $70^\circ\text{C}$ ) towards high temperature.

IER glasses 1 and 2 show two activation energies in the temperature range of about  $590^\circ$  to  $320^\circ\text{C}$ . IER glasses 12, 22 and 13 show linear behaviour in the temperature range  $20^\circ\text{C}$  to  $320^\circ\text{C}$ . The activation energies of the glasses are 0.17, 0.18 and 0.34 respectively. For IER glasses also, the orders of magnitude of surface resistivities are less than that of virgin glasses.

#### 4.3 Switching Studies

I-V characteristics of some IER glasses are shown in figure: 24 . at room temperature. IER glass 1 switches from high resistance state ( $2.2 \times 10^8$  ohm) to low resistance state ( $1.9 \times 10^6$  ohm) at voltage of 250 V. IER glass 4 switches from  $4.5 \times 10^8$  ohm to  $4 \times 10^6$  ohm at 200 V. For IER glass 2 the switching voltage is very low (5.7 volts). The "OFF" state resistance is of the order of  $6 \times 10^8$  ohm and "ON" state resistance is of the order of  $8 \times 10^3$  ohm. There is high instability near switching voltage. After few cycles the "ON" state got stabilised for the glass. Switching characters were also obtained at low temperatures. There was no regular variation of <sup>voltage</sup>  
threshold switching/with temperature.

#### 4.4 Optical Absorption

Optical absorption spectra for few virgin glasses were recorded using Cary-14 spectrometer in the wavelength range of  $2500\text{-}6500\text{ }^{\circ}\text{A}$ . The absorption coefficients were calculated at different wavelengths from the optical spectra using the relation

$$\alpha = \ln \frac{I_0}{I} \frac{1}{x} \text{ cm}^{-1} \quad (4.1)$$

where  $I$  is the transmitted intensity and  $x$  is the thickness of the sample. A plot of  $(\alpha h\nu)^{\frac{1}{2}}$  vs.  $h\nu$  gives the optical absorption edge  $E_{opt}$ , by extrapolating the linear part of the plot as described by Tauc et.al. (66)

From the absorption spectra recorded for the glasses, plots of  $(\alpha h\nu)^{\frac{1}{2}}$  vs.  $h\nu$  were made. Optical gaps thus obtained lie in the range of 2.7 to 3.6 eV, as shown in Fig. 25.

#### 4.5 Differential Thermal Analysis

DTA curves for glass 2 and 3 are shown in Fig. 26. For glass 2 three minima were observed at about 80, 560 and 800°C respectively. A peak was observed at 780°C. For glass 3 a broad dip was observed at 580°C and a small peak at 790°C.

Table 1  
The chemical composition of the glasses

Glass No.	Composition in mole %					
	Na <sub>2</sub> O	B <sub>2</sub> O <sub>3</sub>	Bi <sub>2</sub> O <sub>3</sub>	Sb <sub>2</sub> O <sub>3</sub>	SiO <sub>2</sub>	K <sub>2</sub> O
1	10	18	10	2	60	-
2	10	15	10	5	60	-
3	10	16	5	5	64	-
4	10	15	5	10	60	-
5	10	18	2	10	60	-
11	5	21	5	5	64	-
12	3	22	5	5	64	1
13	1	23	5	5	64	2
21	5	20	5	10	60	-
22	3	21	5	10	60	1
23	1	22	5	10	60	2

Table 2

Activation energy E calculated from  $\log \sigma'$  vs.  $1/T$  plots for different regions of the curves for glasses studied, as computed using method of least squares

Glass No.	Fig. No.	Inverse temperature range ( $1/T$ )		Region marked on the graph	Activation energy eV	Standard deviation eV
<u>I Bulk resistivity</u>						
1	2	1.72	2.0	(a)	0.47	0.10
		2.4	3.4	(b)	0.53	0.04
		1.6	2.6	(c)	1.10	0.02
2	3	1.7	2.4	(a)	0.26	0.02
		2.5	3.4	(b)	0.91	0.04
3	4	1.5	2.9	(a)	0.31	0.01
		3.9	5.4	(b)	0.23	0.01
4	5	1.7	2.4	(a)	0.28	0.02
		2.5	3.4	(b)	0.79	0.05
5	6	1.7	2.1	(a)	0.13	0.03
		2.4	3.4	(b)	0.67	0.04
		1.7	2.7	(c)	1.08	0.03
12	7	1.5	2.1	(a)	0.55	0.01
21	8	1.4	1.8	(a)	1.42	0.09
		2.0	2.5	(b)	1.11	0.11
23	9	1.4	2.2	(a)	0.77	0.06
		2.2	3.0	(b)	0.40	0.02

Table 2 (Continued)

Glass No.	Fig. No.	Inverse temperature range ( $1/T$ )		Region marked on the graph	Activation energy eV	Standard deviation eV
		From	To			

II Surface resistivityA. Virgin glasses

1	11	1.4	2.4	(a)	1.07	0.03
3	11	1.4	2.4	(a)	1.03	0.08
4	11	1.4	2.6	(a)	1.07	0.02
5	11	1.4	2.6	(a)	0.96	0.03
11	12	1.5 2.5	2.5 3.2	(a) (b)	-0.81 -0.51	0.03
12	12	1.4 2.5	2.0 3.2	(a) (b)	1.04 0.50	0.02
13	12	1.4 2.5	2.0 3.2	(a) (b)	1.05 0.50	

B. Reduced glasses

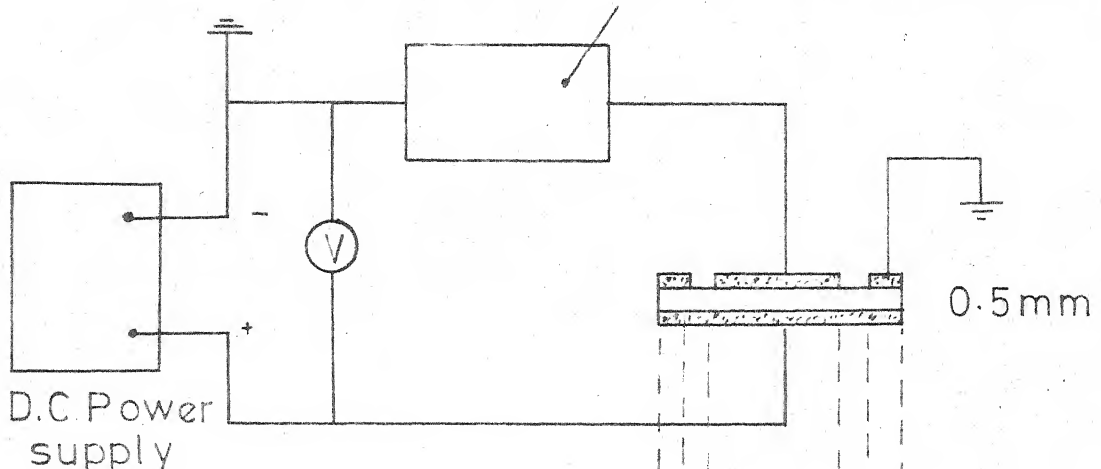
2	13	1.8	3.2	(b)	0.21	0.01
3	13	1.7 2.3 1.7	2.3 3.2 2.7	(a) (b) (c)	0.55 0.28 0.54	0.03 0.02 0.02
11	14	1.7	3.1	(b)	0.22	0.05
12	14	1.7	3.1	(b)	0.19	0.01
13	15	1.7 2.1	2.2 2.8	(a) (b)	0.73 0.47	0.07 0.20

CERI-KAL  
Acc. No. 47068

Table 2 (Continued)

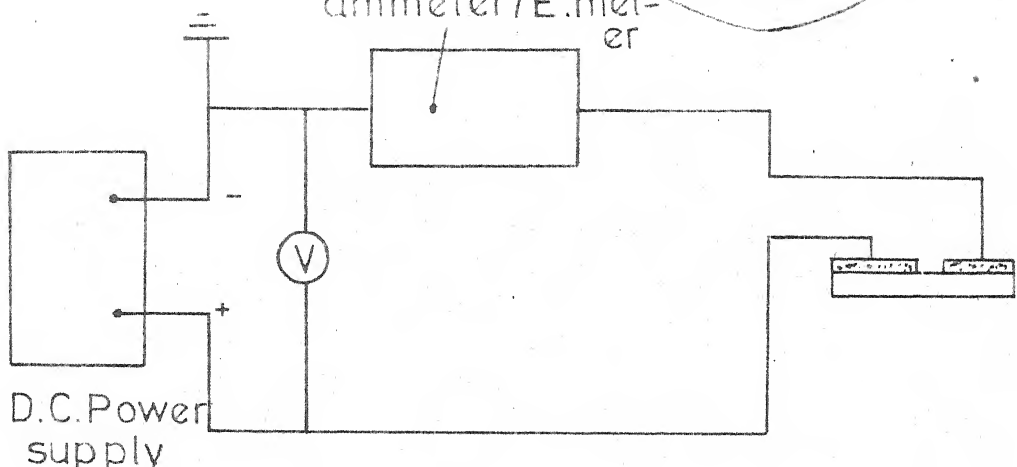
Glass No.	Fig. No.	Inverse temperature range ( $1/T$ )		Region marked on the graph	Activation energy eV	Standard deviation eV
		From	To			
<u>C. Ion-exchanged and reduced glasses</u>						
1	16	1.8 3.0	3.0 5.5	(a) (b)	0.66 0.08	0.02 0.03
2	17	2.0 3.5	3.0 5.0	(a) (b)	0.15 0.08	0.02 0.004
3	18	2.0 2.7	2.6 3.2	(a) (b)	0.69 0.87	0.04 0.25
4	19	3.2	4.6	(b)	0.13	0.01
5	20	1.9 3.3	2.5 3.8	(a) (b)	0.64 0.77	0.02 0.09
11	21	2.4 2.2	3.3 3.1	(b) (a)	0.58 0.77	0.04 0.01
12	22	1.8	3.2	(b)	0.17	0.01
13	22	1.8	3.2	(b)	0.34	0.07
21	23	1.8	3.0	(b)	0.57	0.03
22	22	1.7	3.2	(b)	0.19	0.01

Digital picoammeter/E.meter



(a)

Digital pico-  
ammeter/E.meter



(b)

FIG.1 SCHEMATIC CIRCUIT DIAGRAM FOR

(a) Bulk resistivity measurement

(b) Surface resistivity measurement

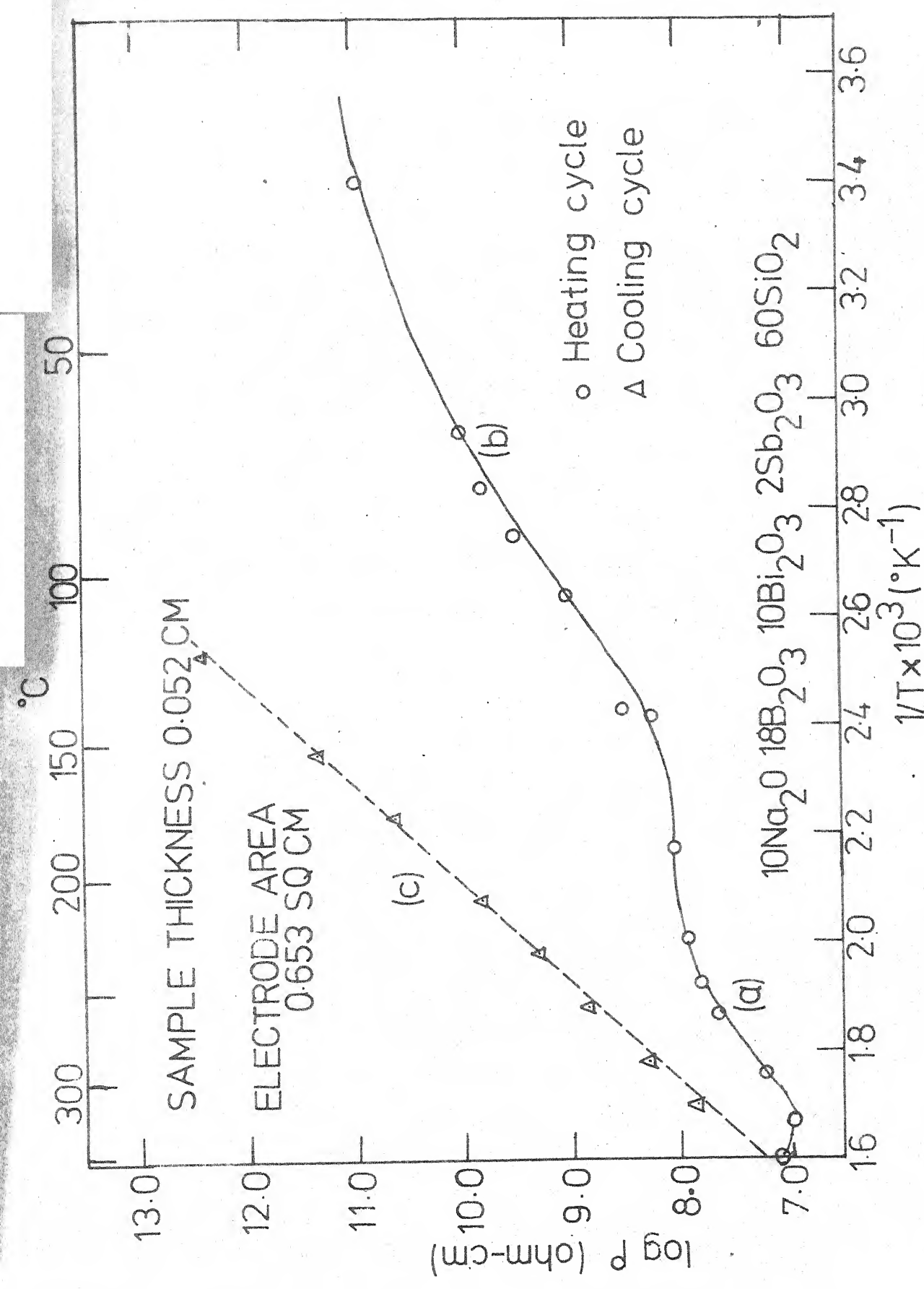


FIG.2 VARIATION OF BULK RESISTIVITY WITH TEMPERATURE  
 FOR GLASS NO.1

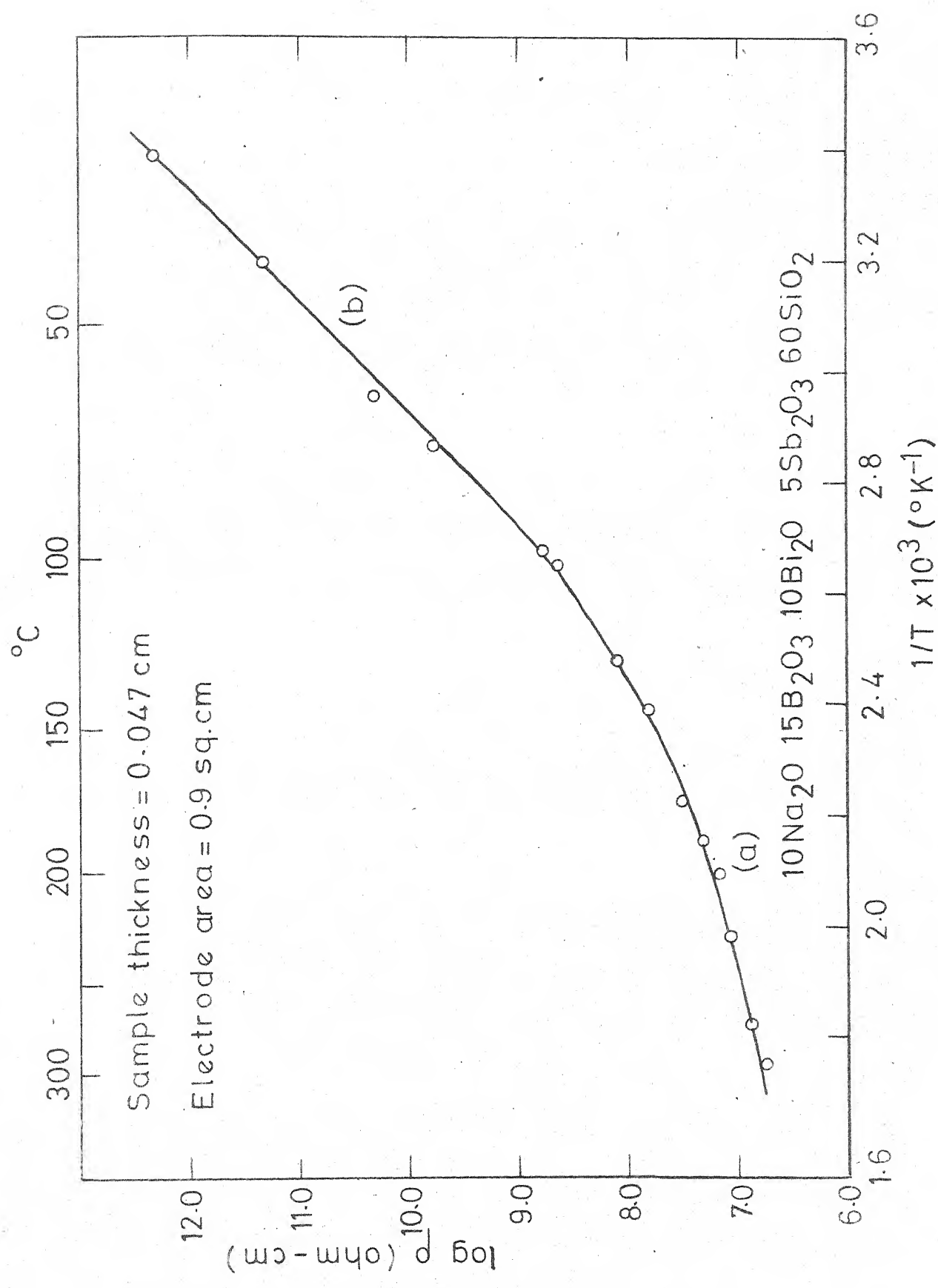


Fig. 3 Variation of bulk resistivity with temperature for glass 2.

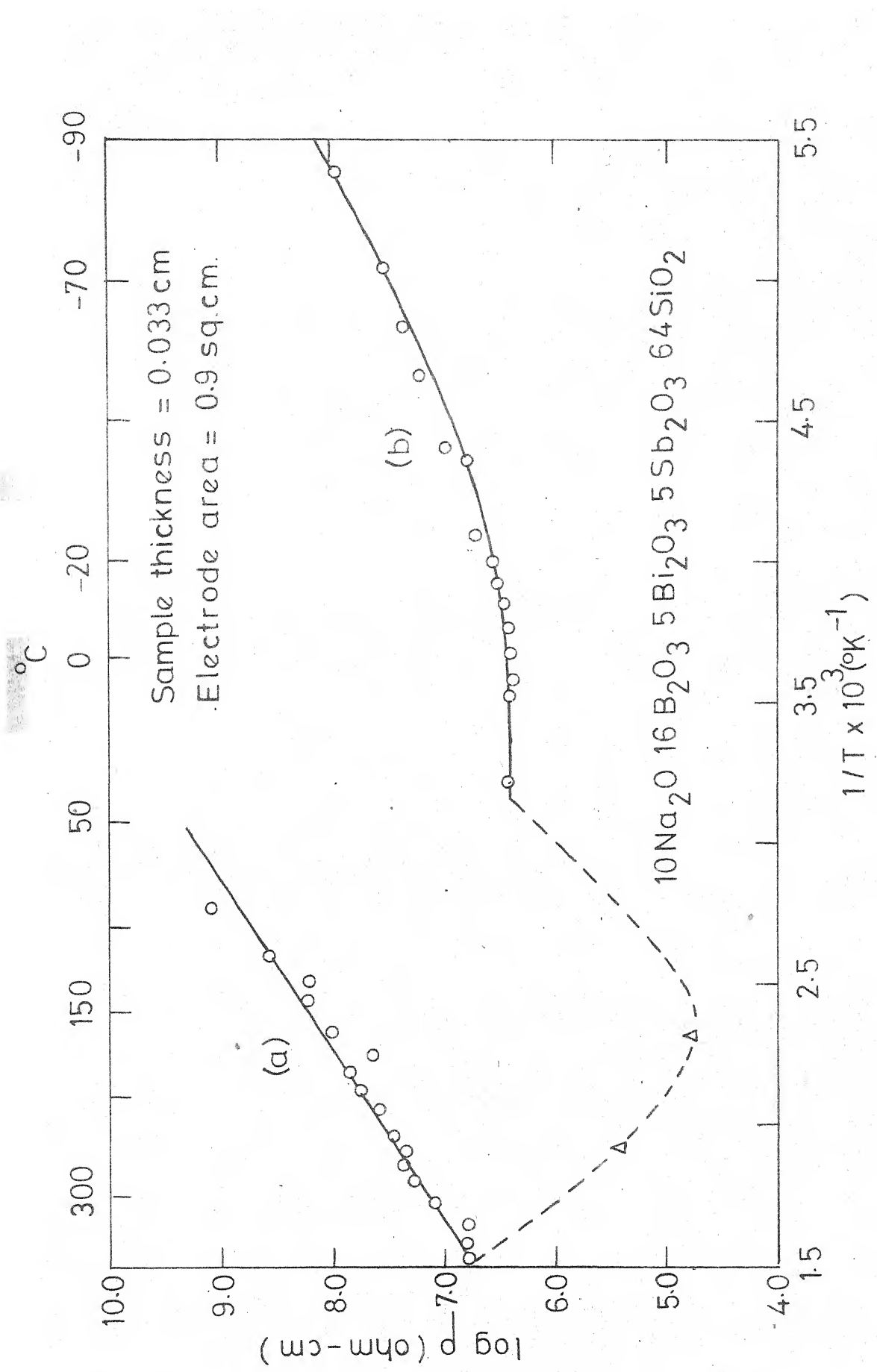


Fig. 4 Variation of bulk resistivity with temperature for glass 3.

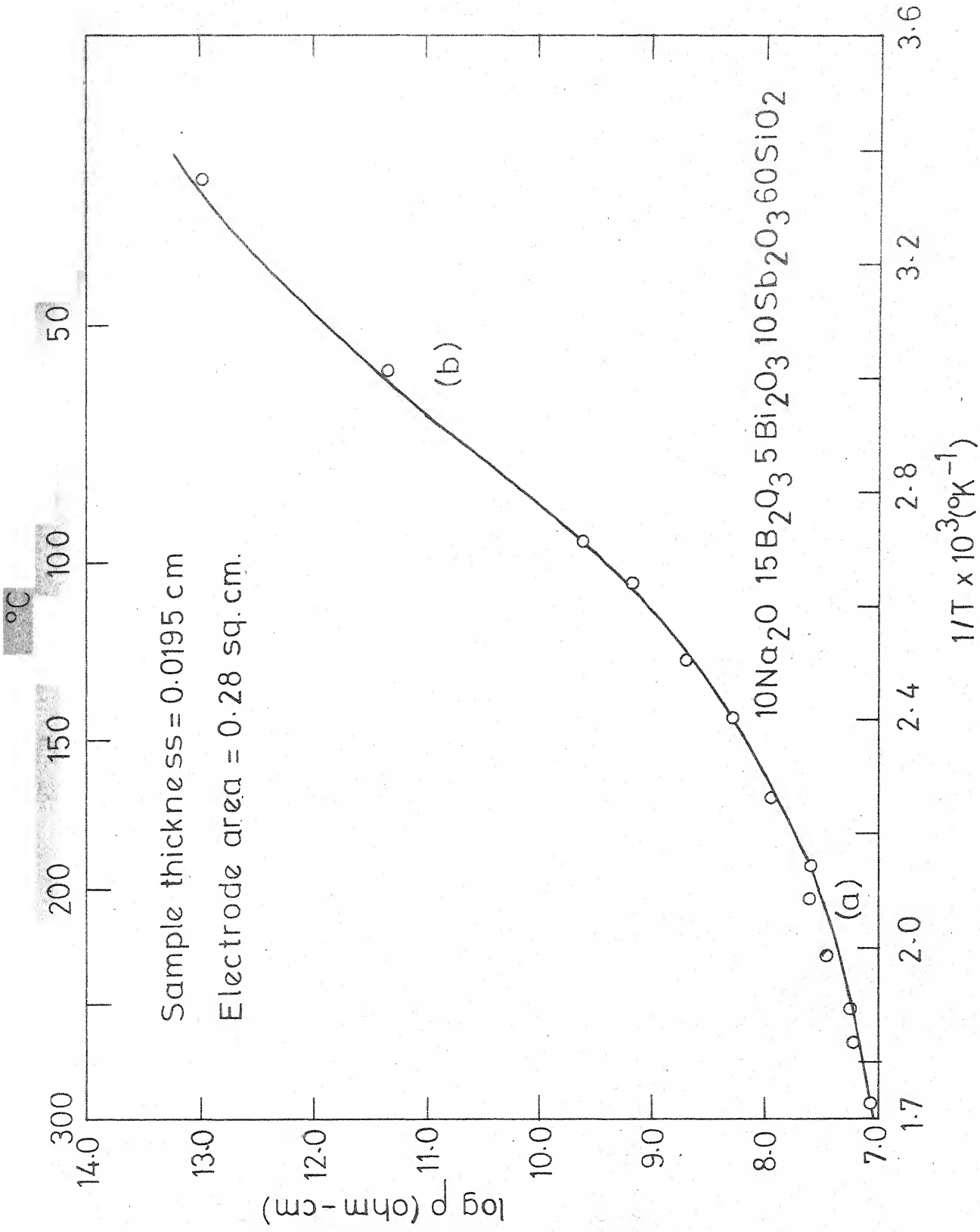


Fig. 5 Variation of bulk resistivity with temperature for glass 4.

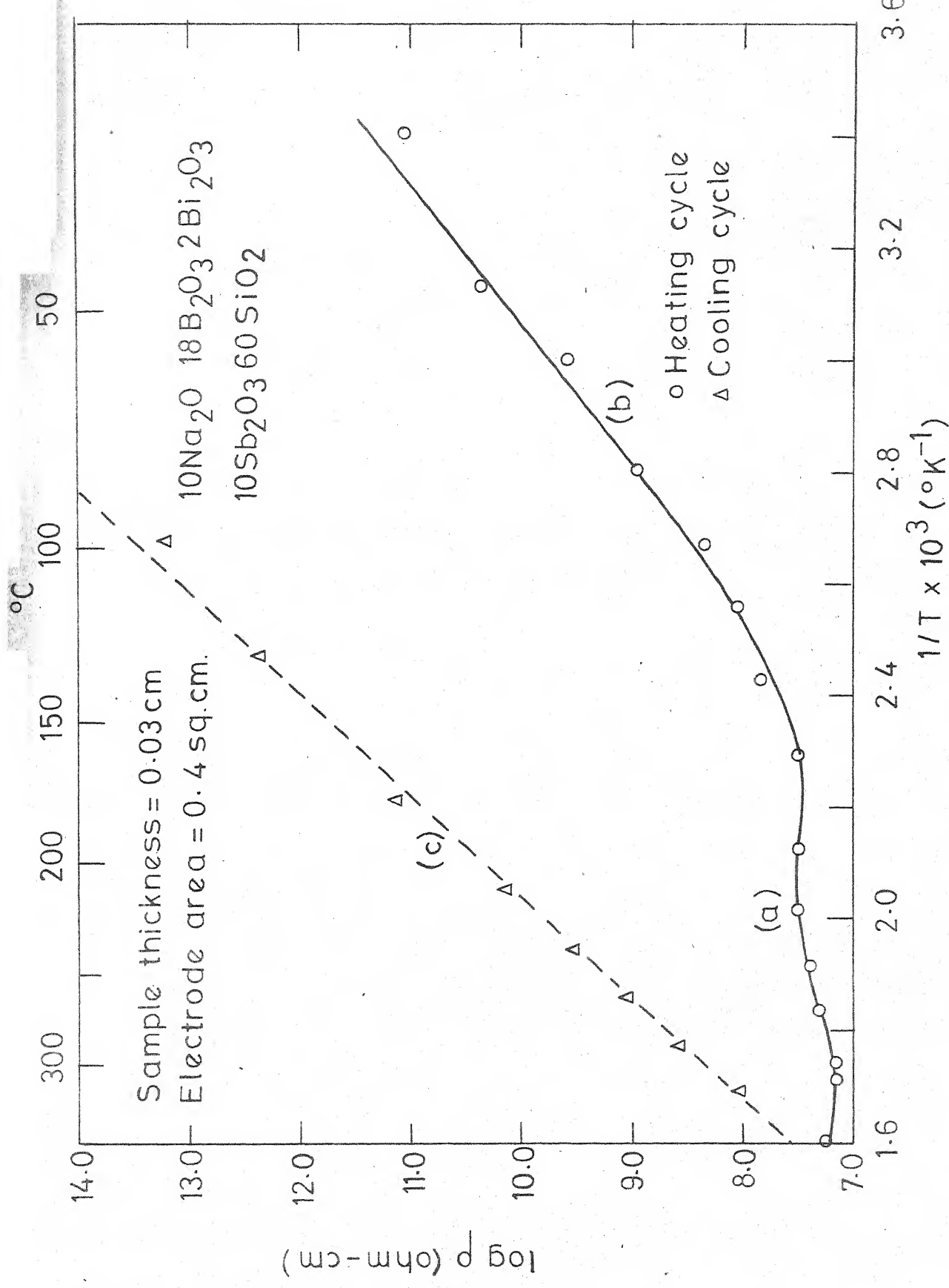


Fig. 6 Variation of bulk resistivity with temperature for glass 5.

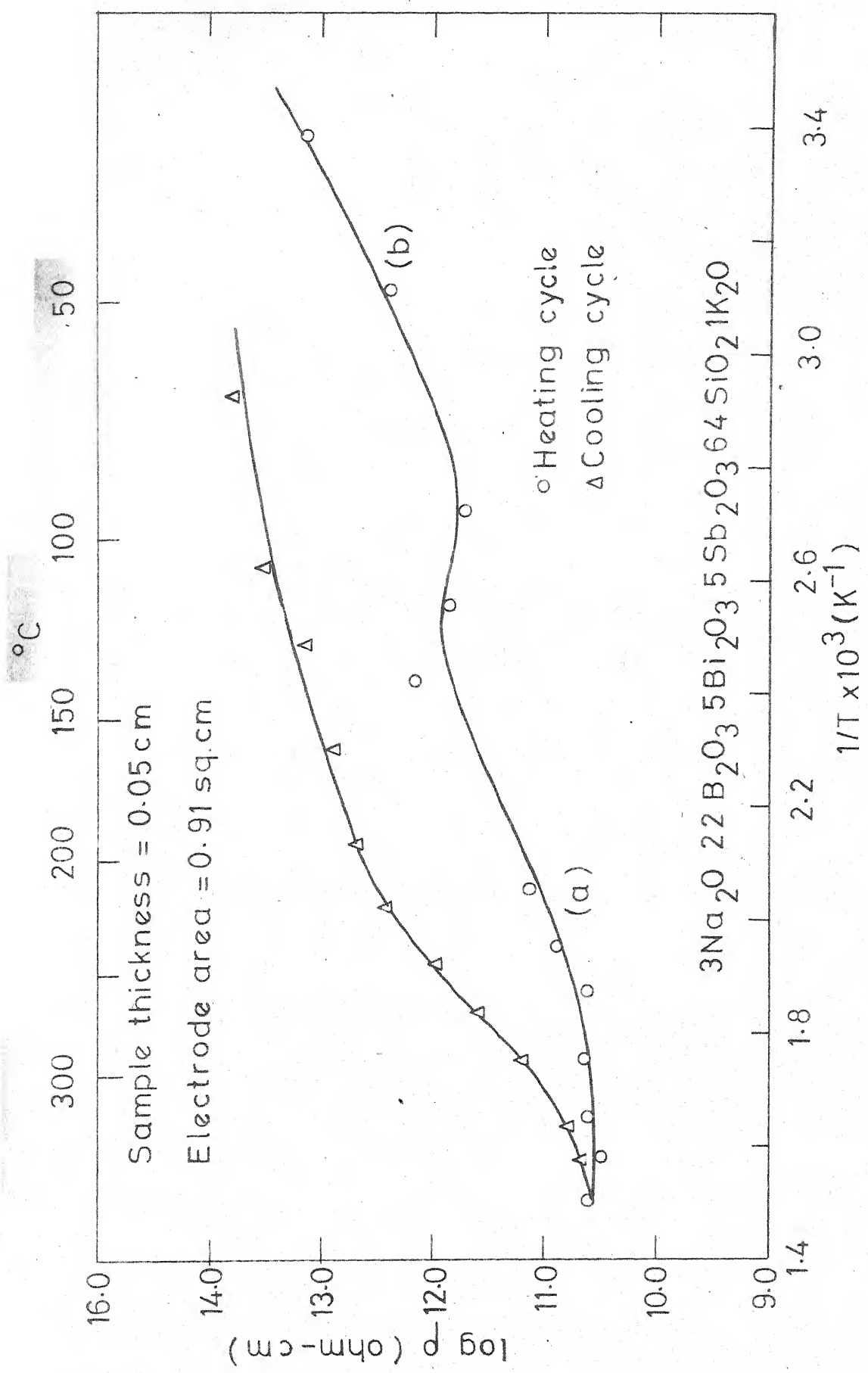


Fig. 7 Variation of bulk resistivity with temperature for glass 12.

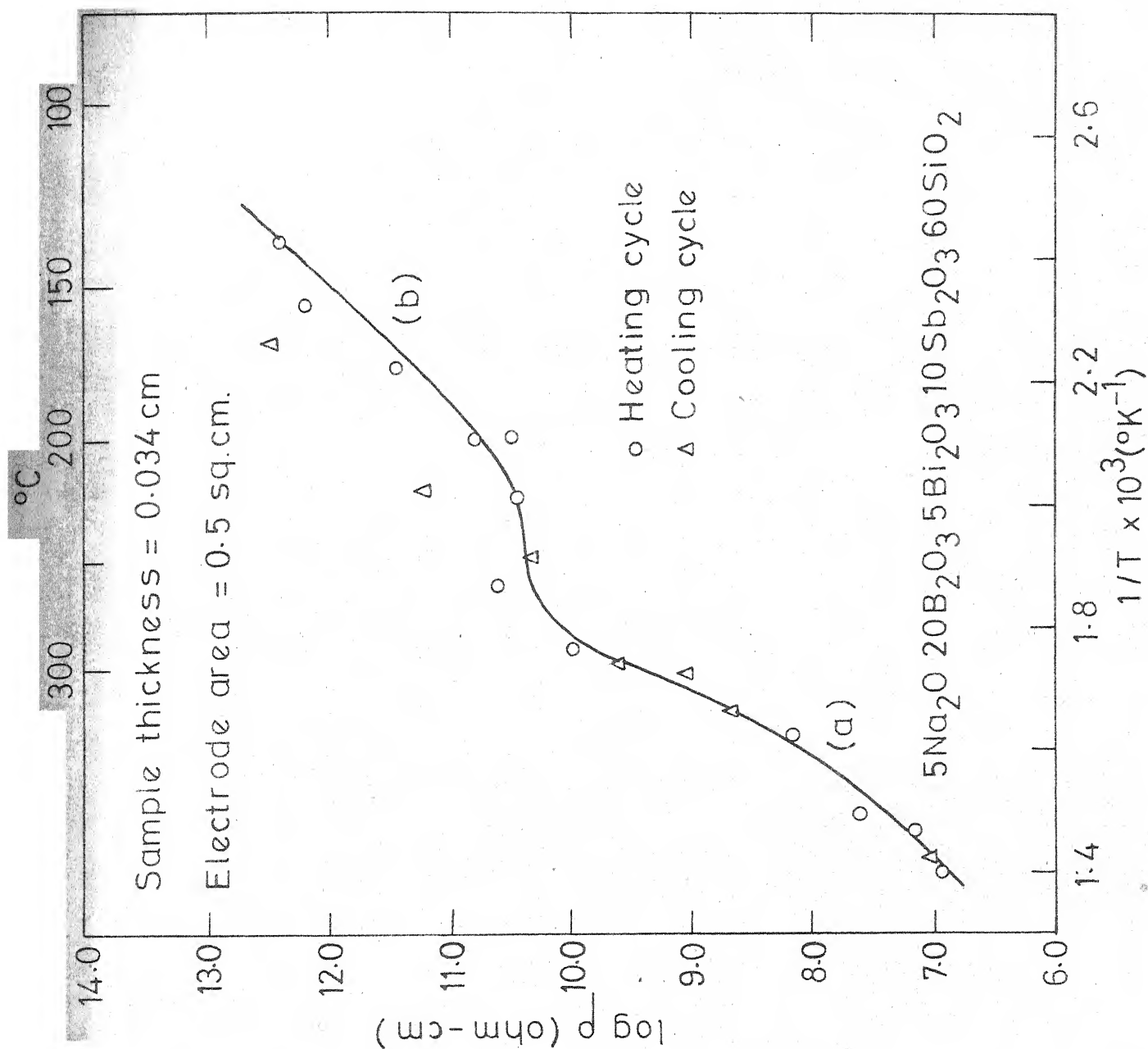


Fig. 8 Variation of bulk resistivity with temperature for

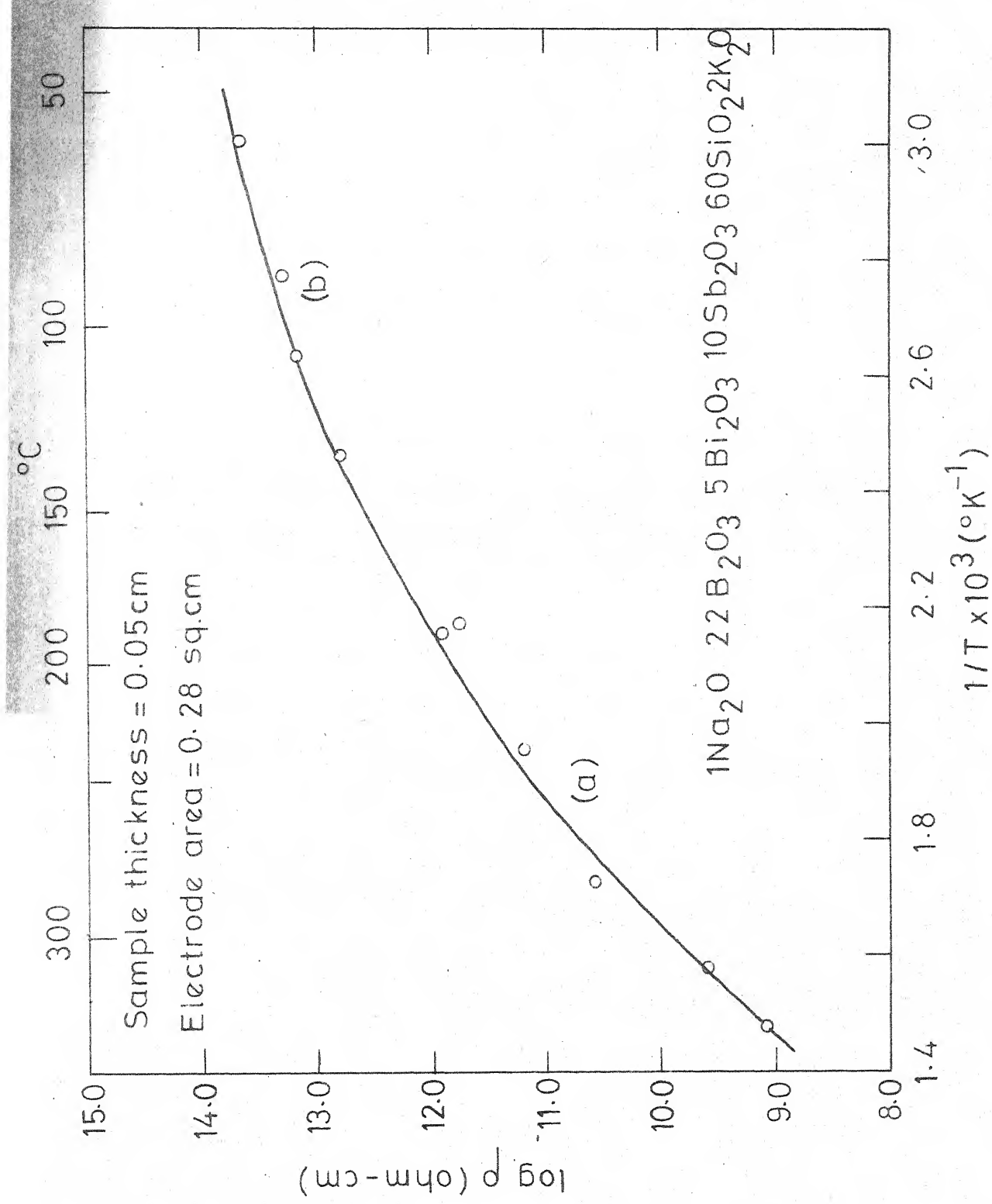


Fig. 9 Variation of bulk resistivity with temperature for glass 23.

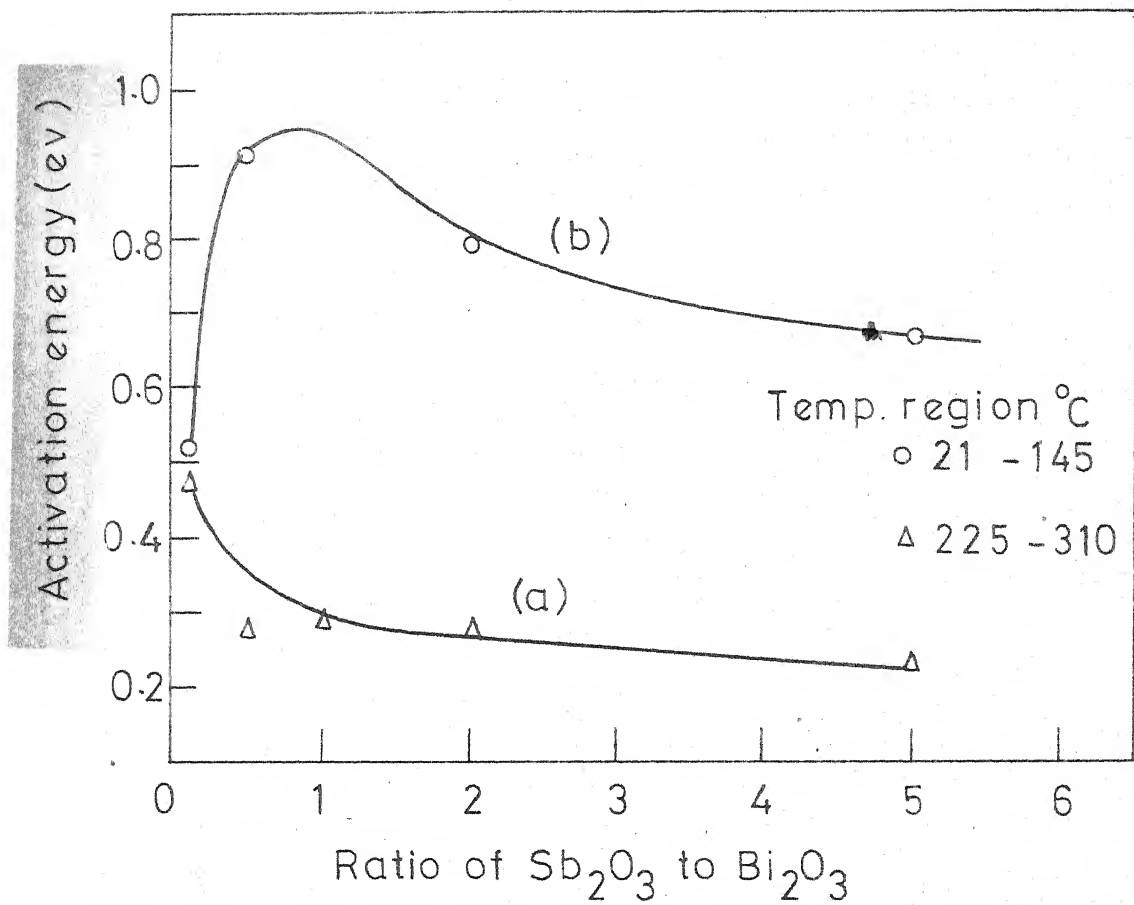


Fig. 10 Variation of activation energy with ratio of concentration of  $Sb_2O_3$  to  $Bi_2O_3$ .

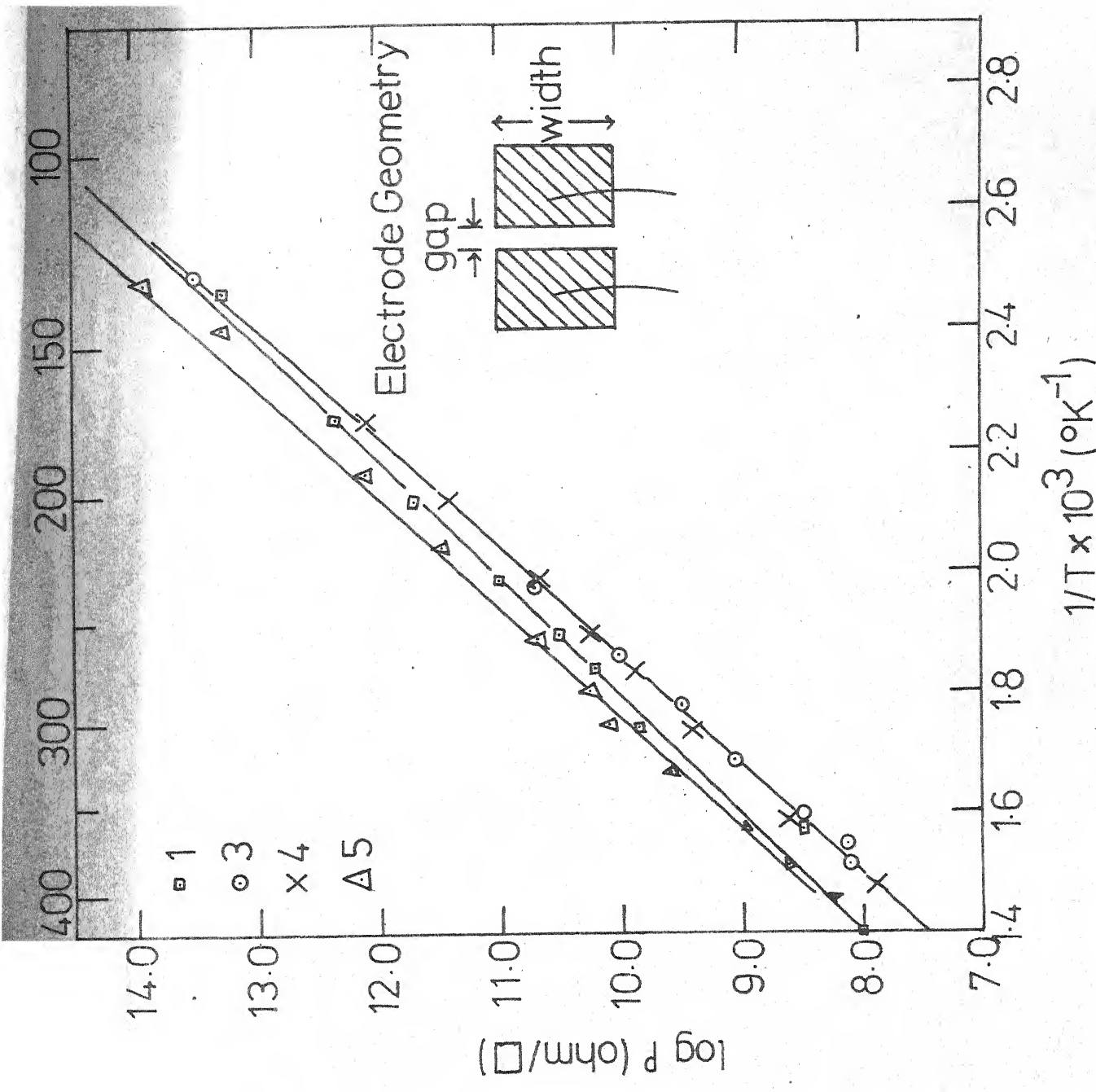


Fig.11 VARIATION OF SURFACE RESISTIVITY OF VIRGIN GLASSES WITH TEMPERATURE

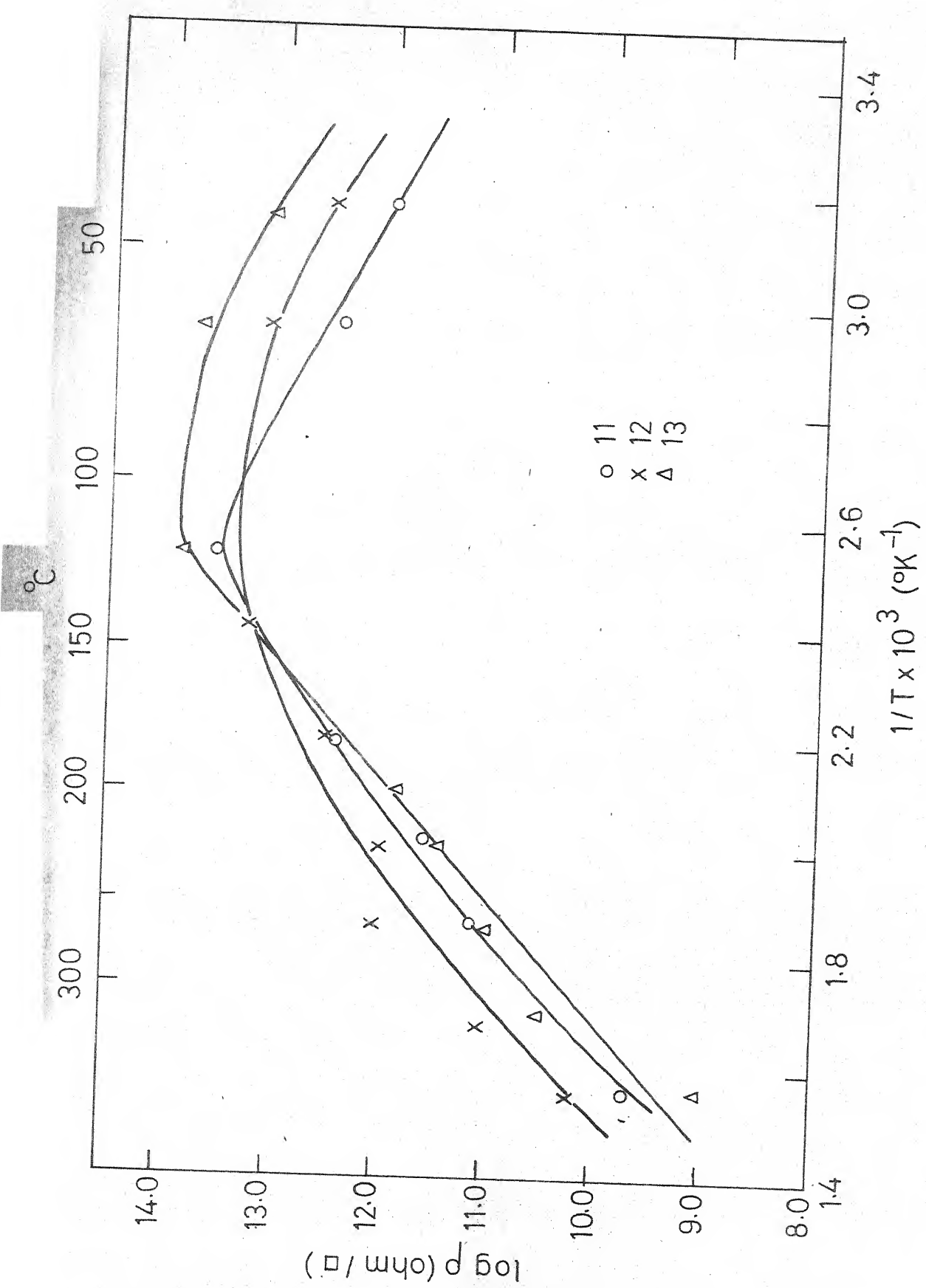


Fig. 12 Variation of surface resistivities of virgin glasses 11, 12 and 13 with temperature

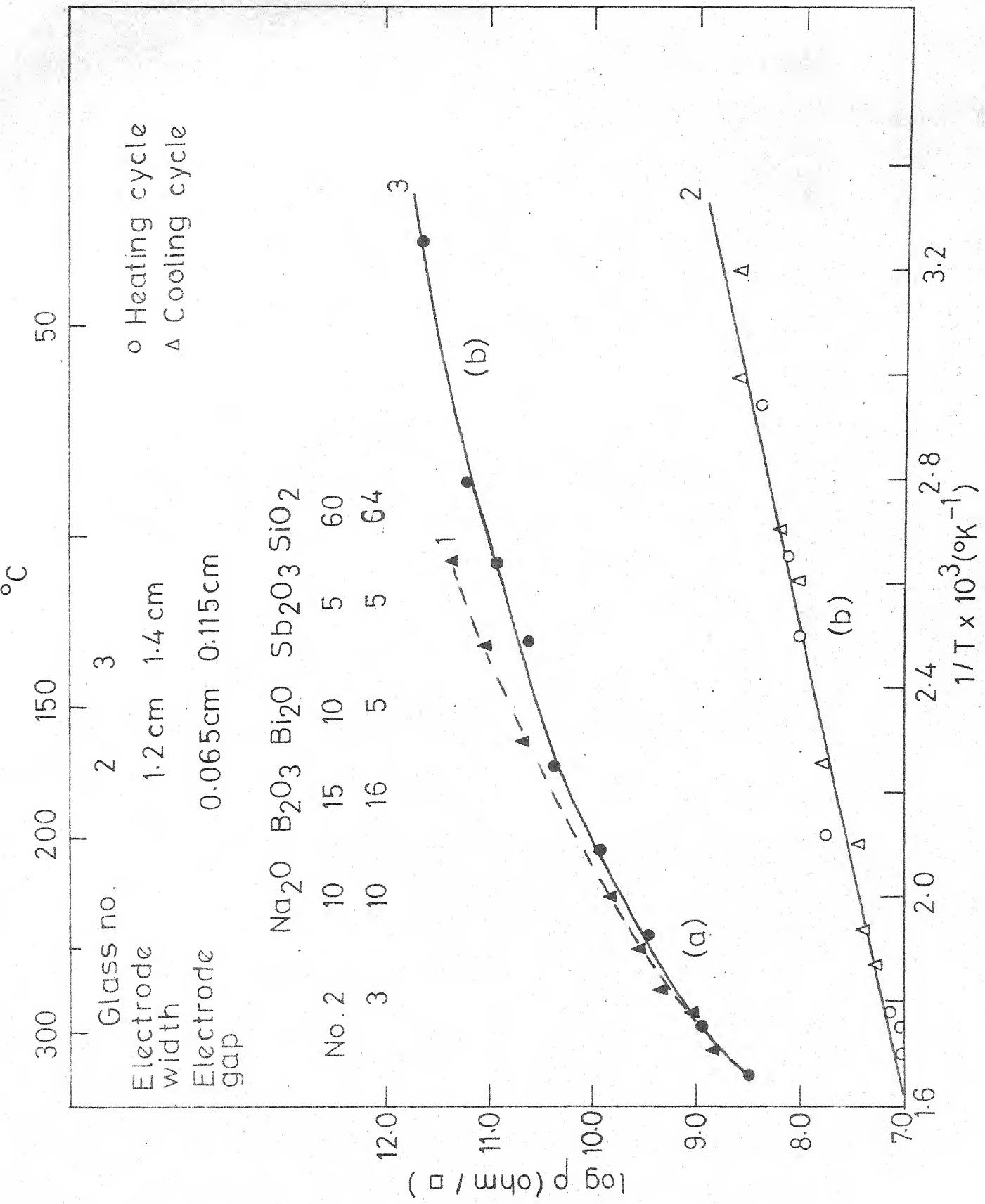


FIG. 13 Variation of surface resistivities of reduced glass 2 & 3 with temperature

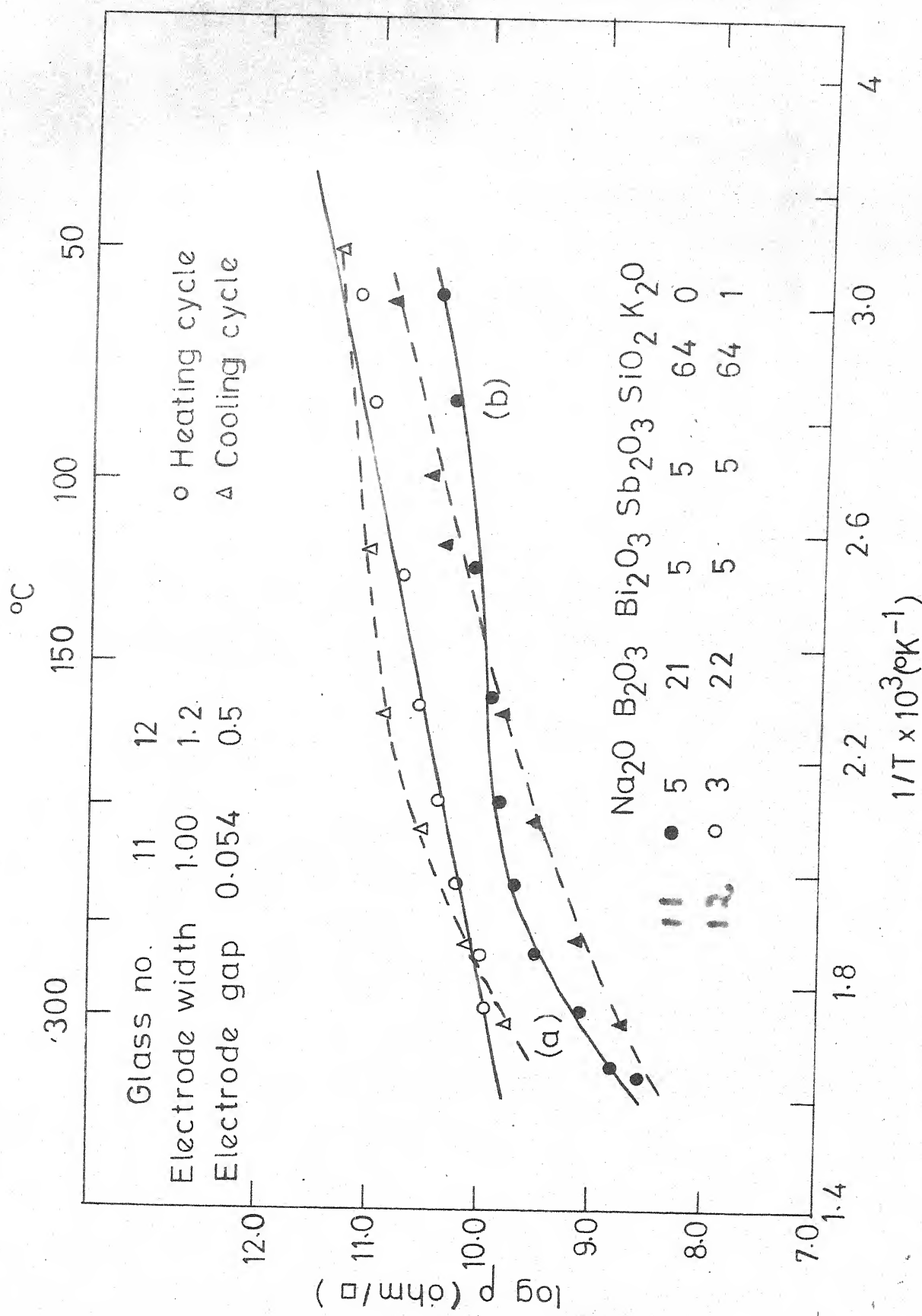


Fig. 14 Variation of surface resistivity of reduced glasses 11 & 12 with temperature

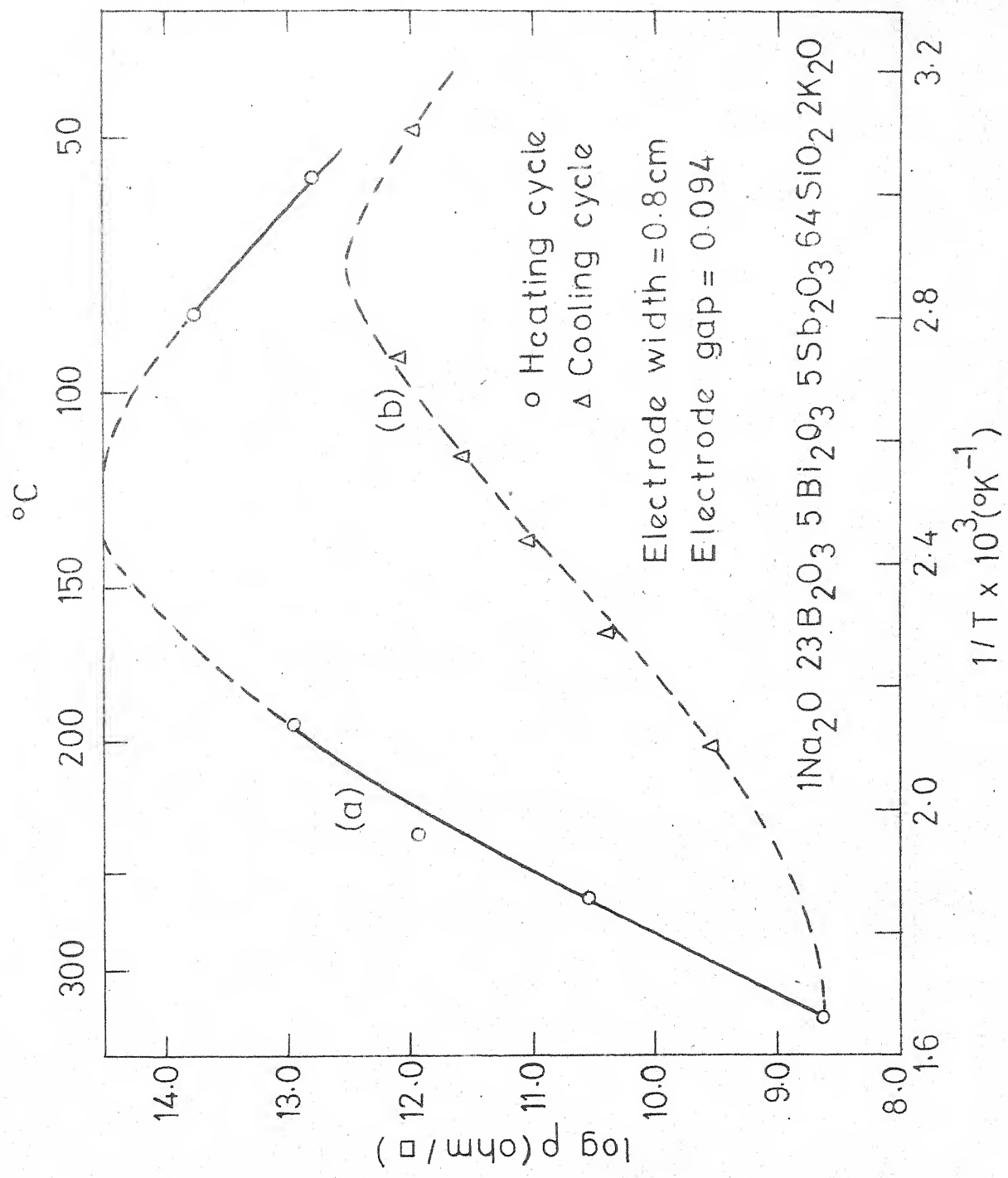


Fig. 15 Variation of surface resistivity of reduced glass 13 with temperature

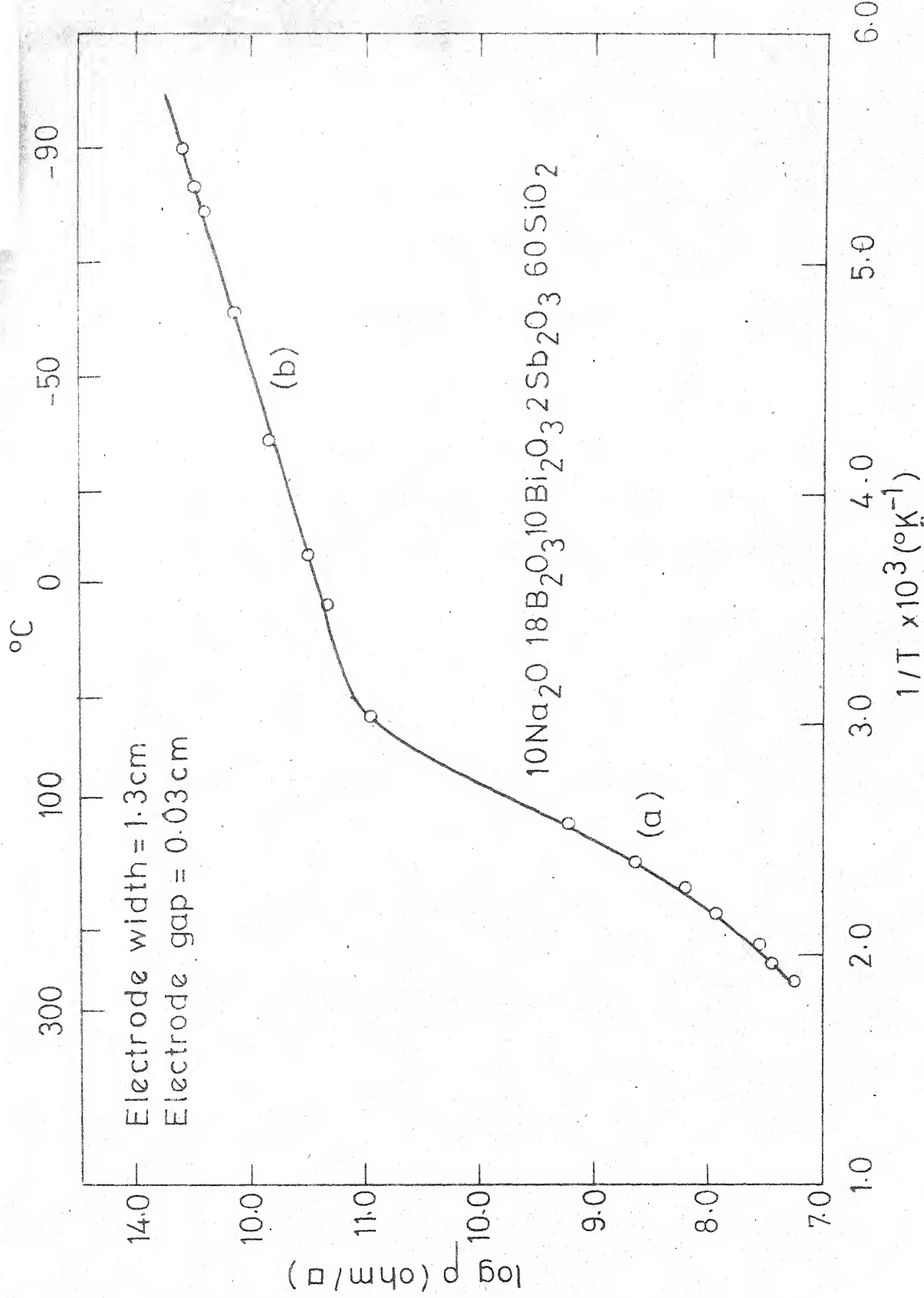
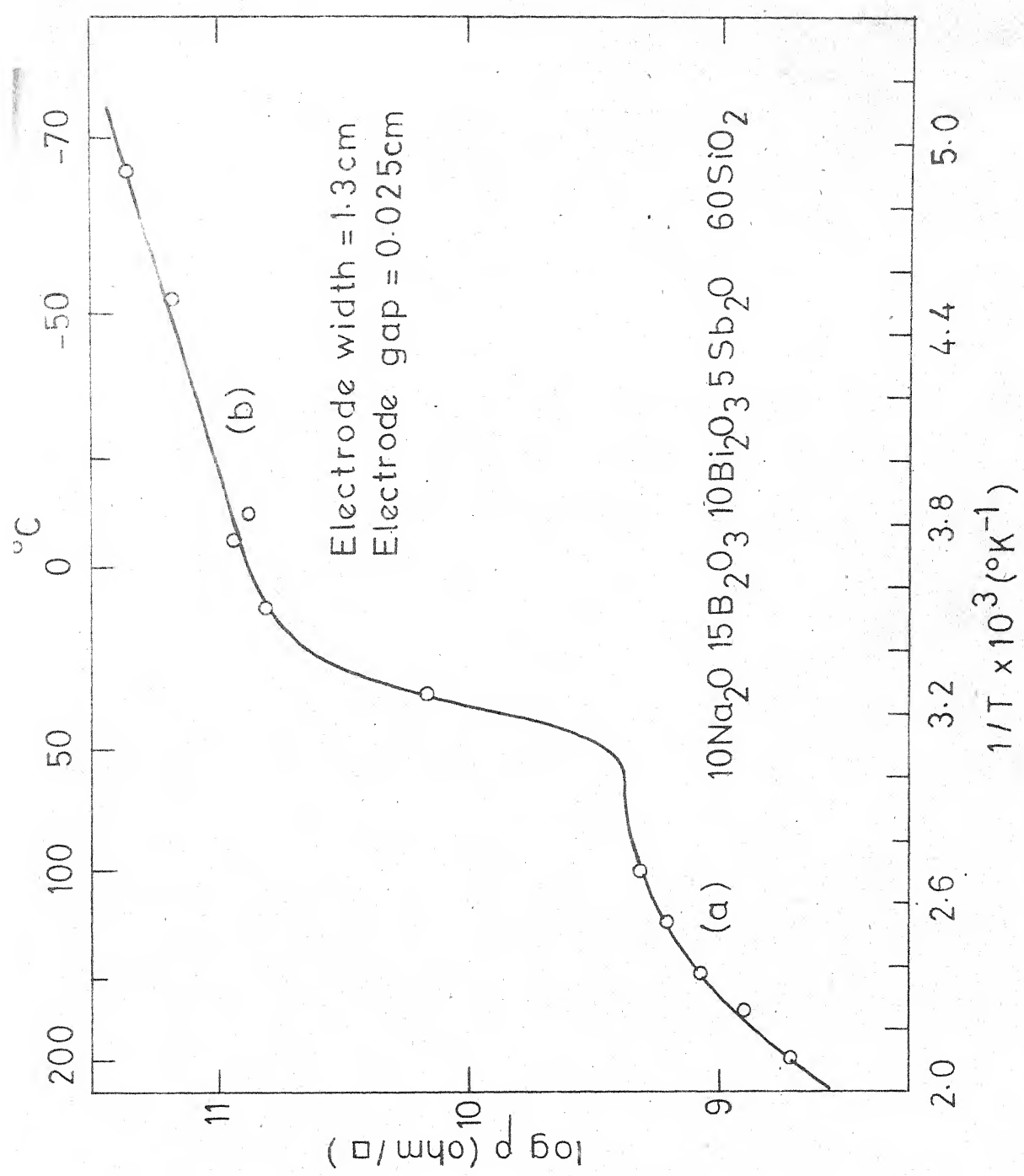
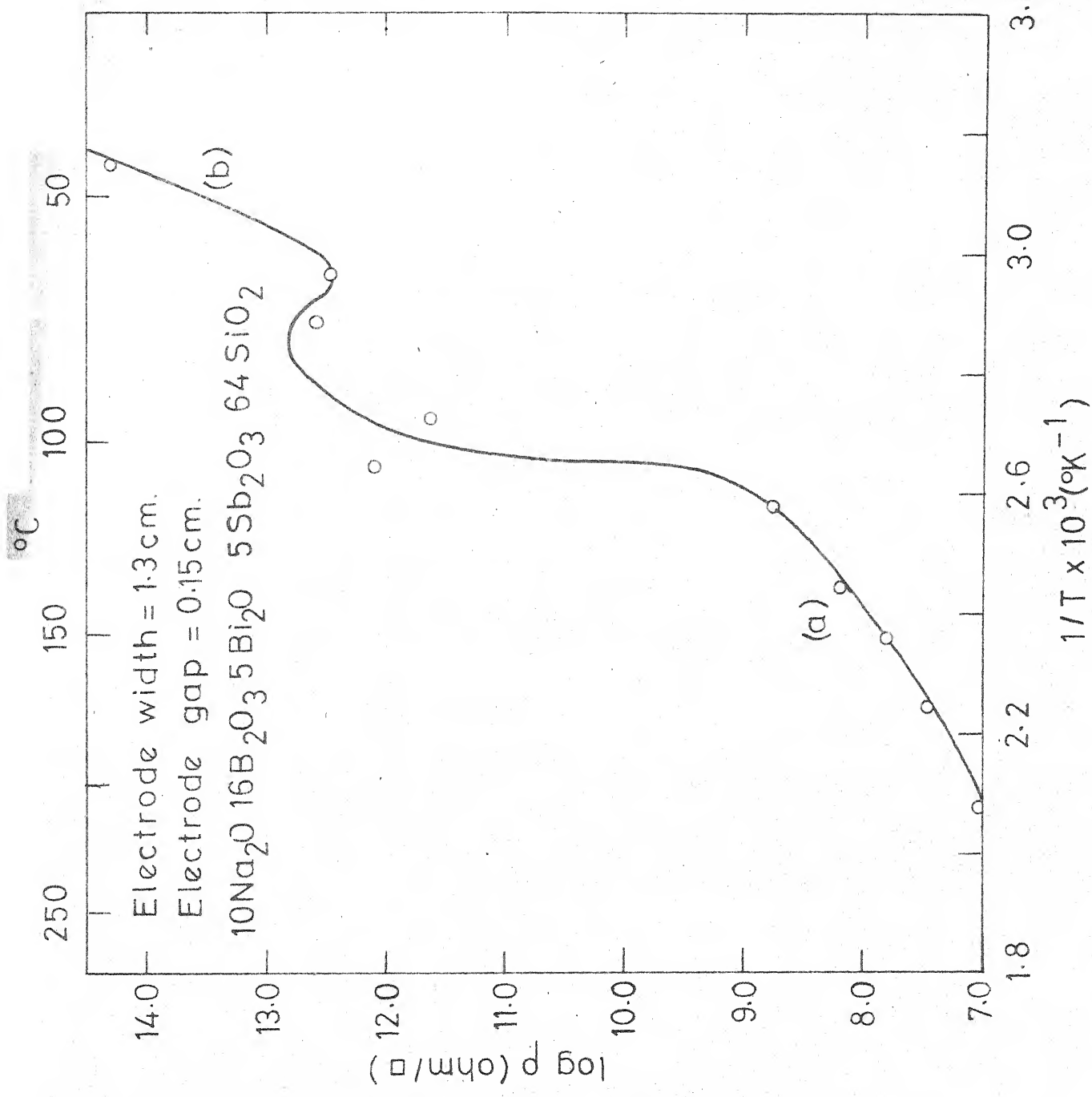


Fig. 16 Variation of surface resistivity of ion-exchanged and reduced glass 1





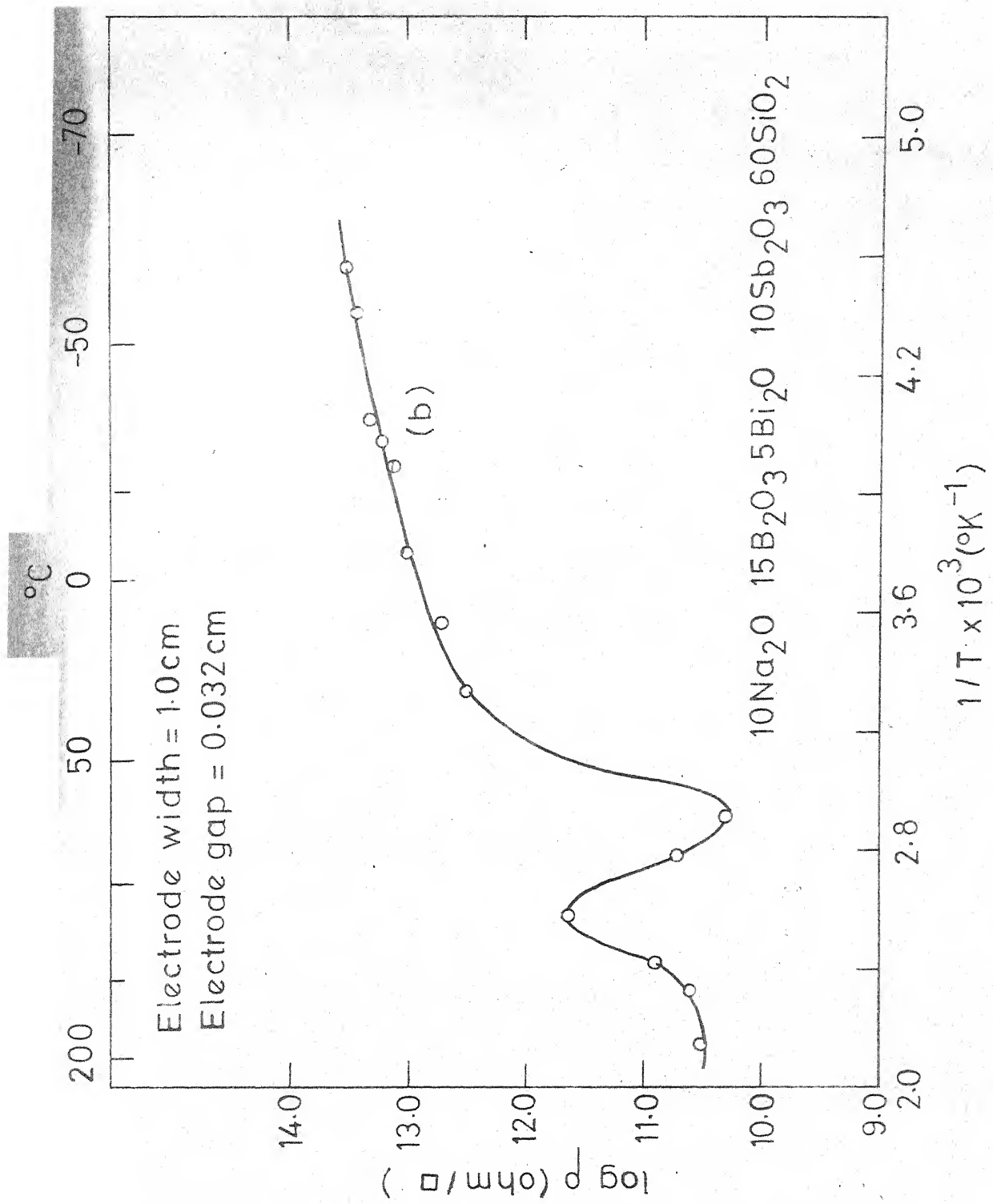


Fig. 19 Variation of surface resistivity of IER glass 4 with temperature

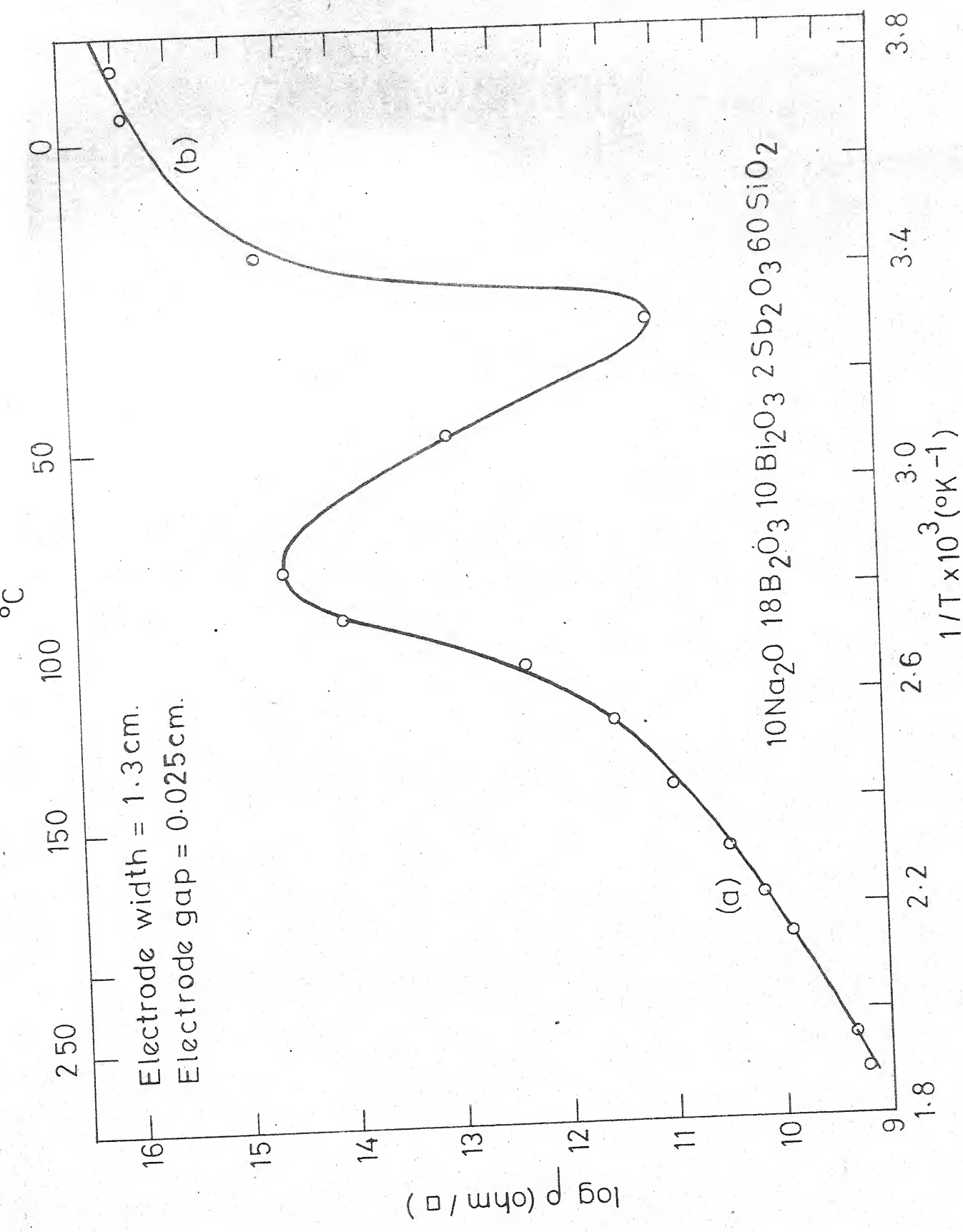


Fig. 20 Variation of surface resistivity of TER glasses 5 with temperature

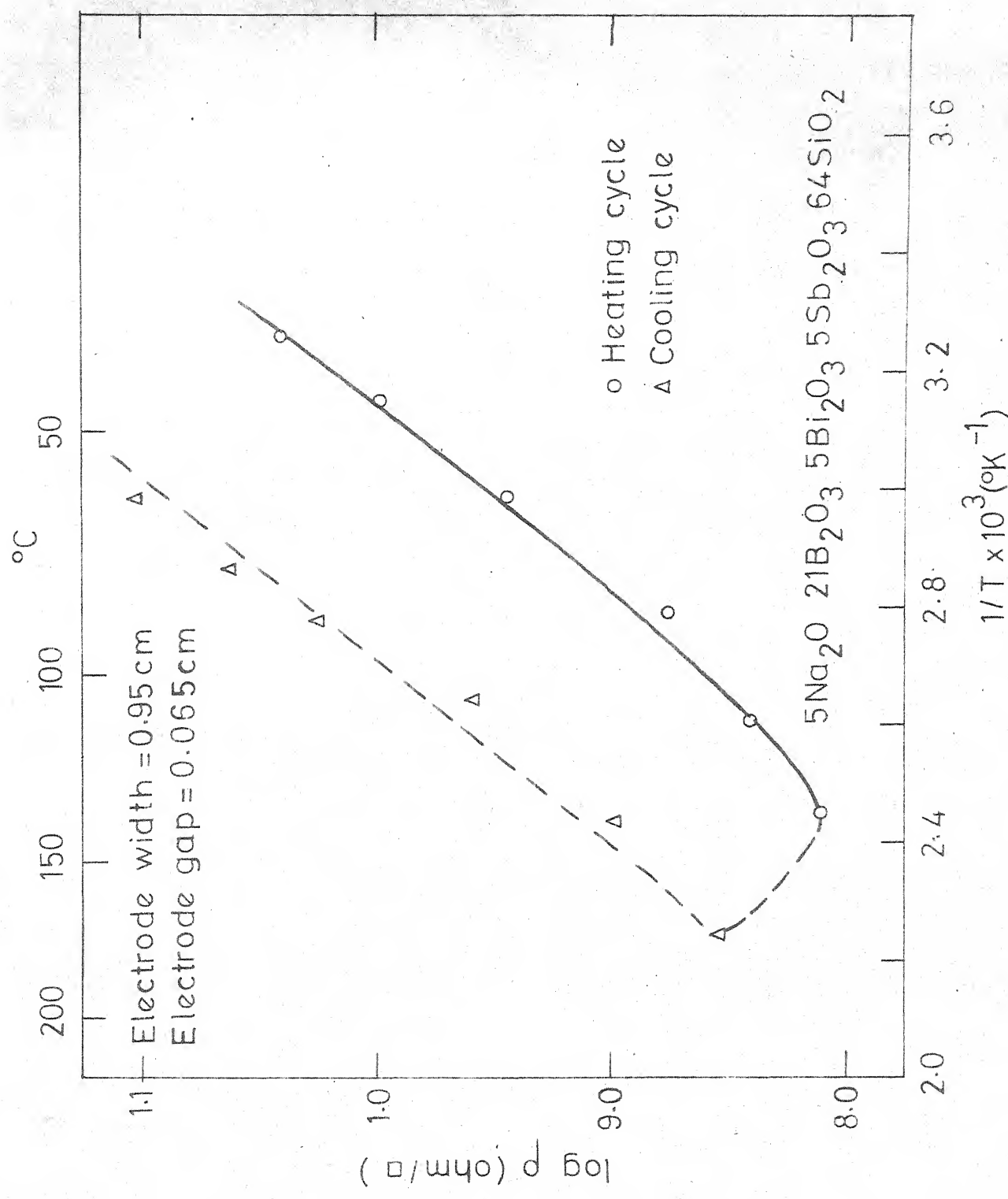


Fig. 21 Variation of surface resistivities of IER glass 11 with temperature

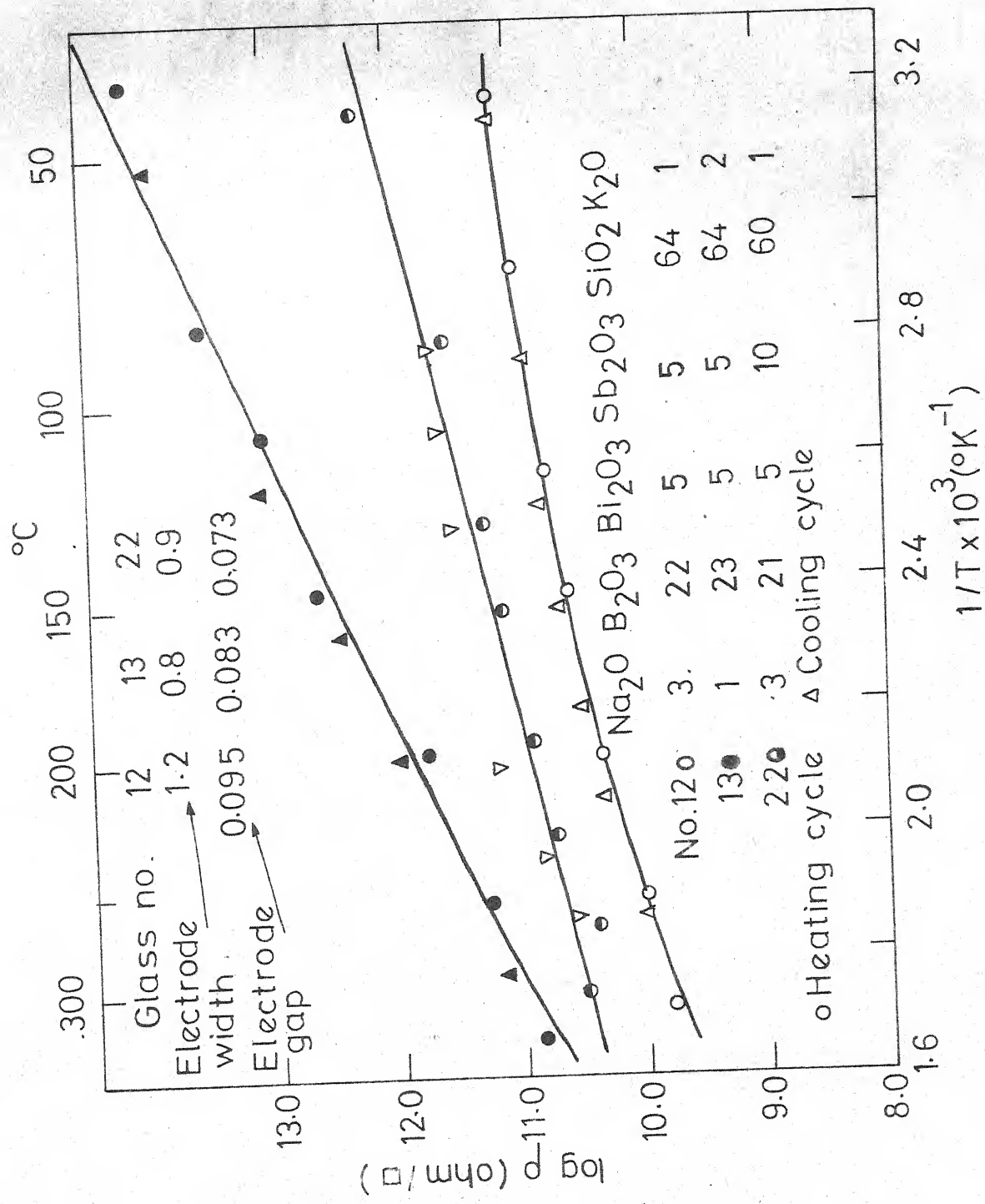


Fig. 22 Variation of surface resistivity of IER glass 12, 13 & 22 with temperature

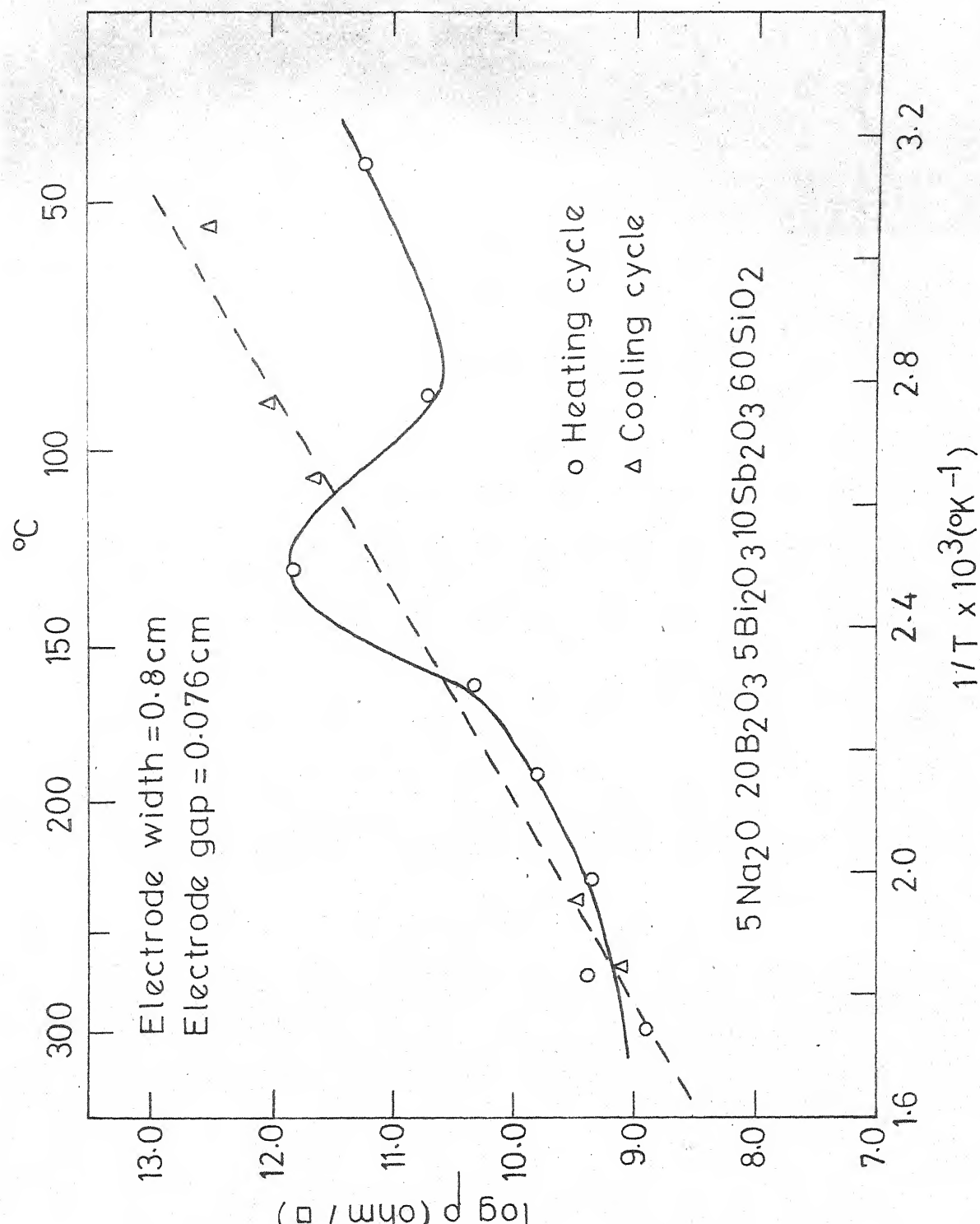


Fig. 23 Variation of surface resistivity of IER glass 21 with temperature

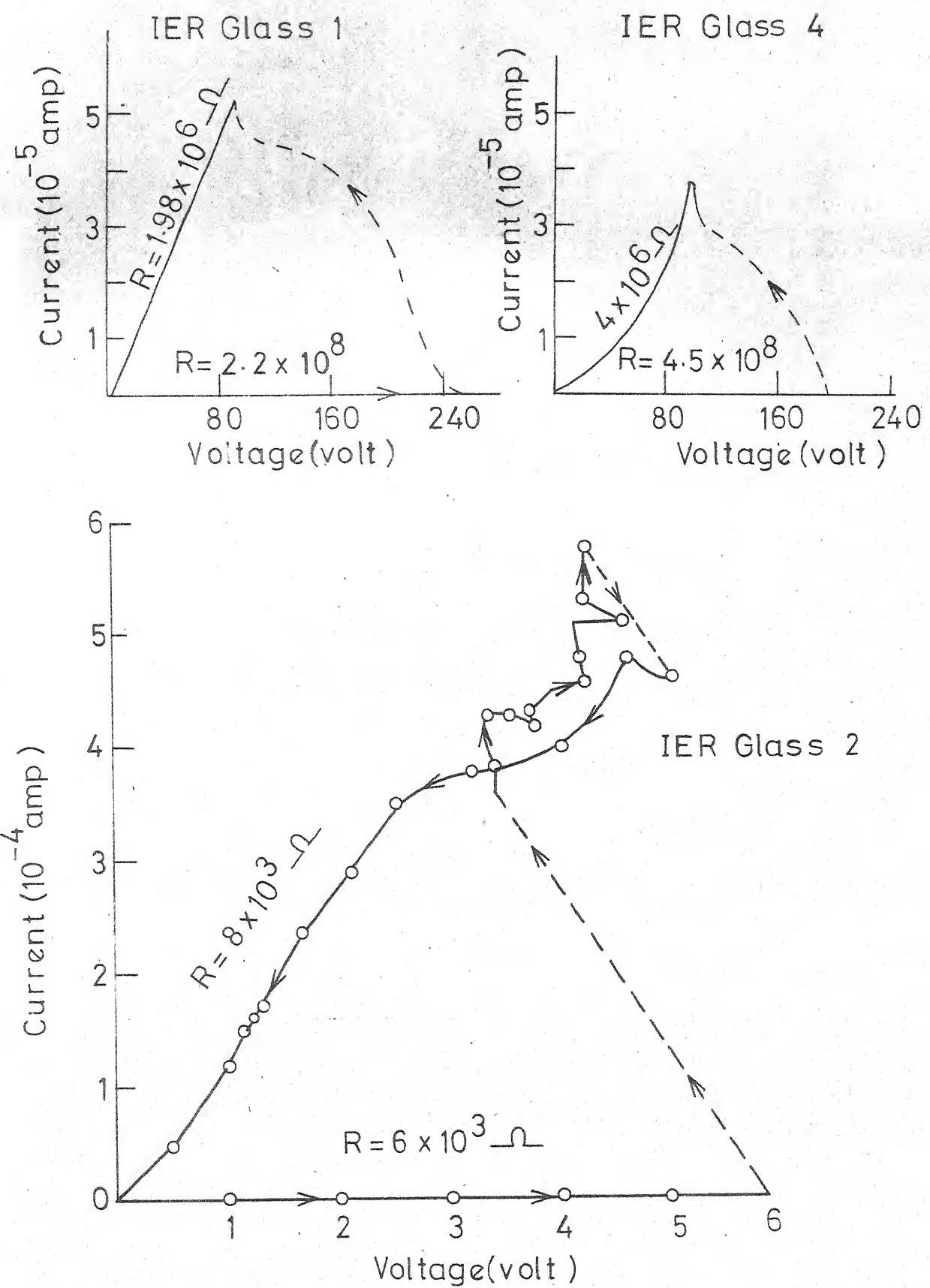


Fig. 24 Switching characteristics of IER glasses 1, 2 & 4.

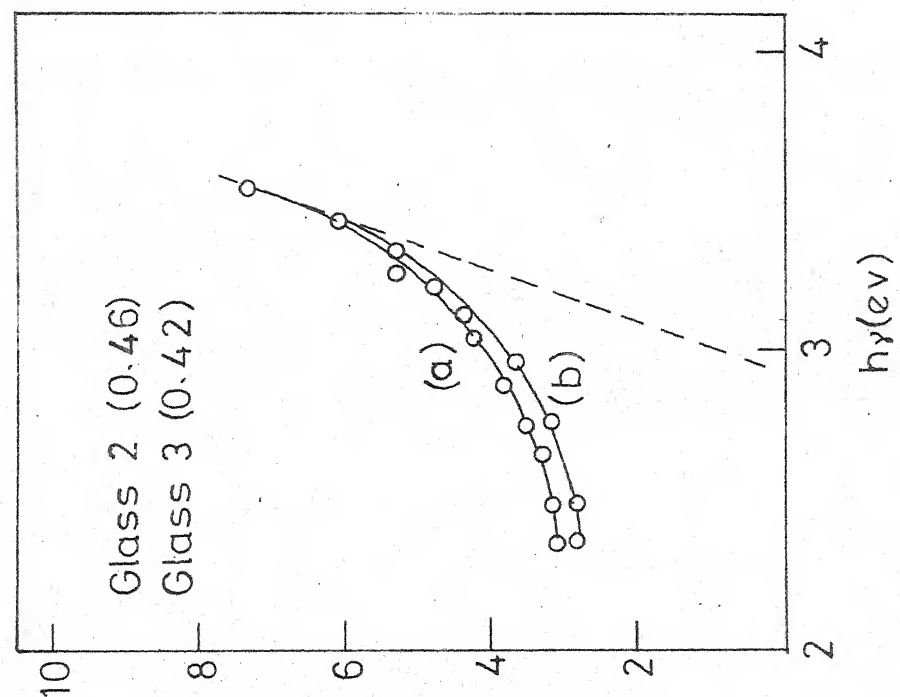
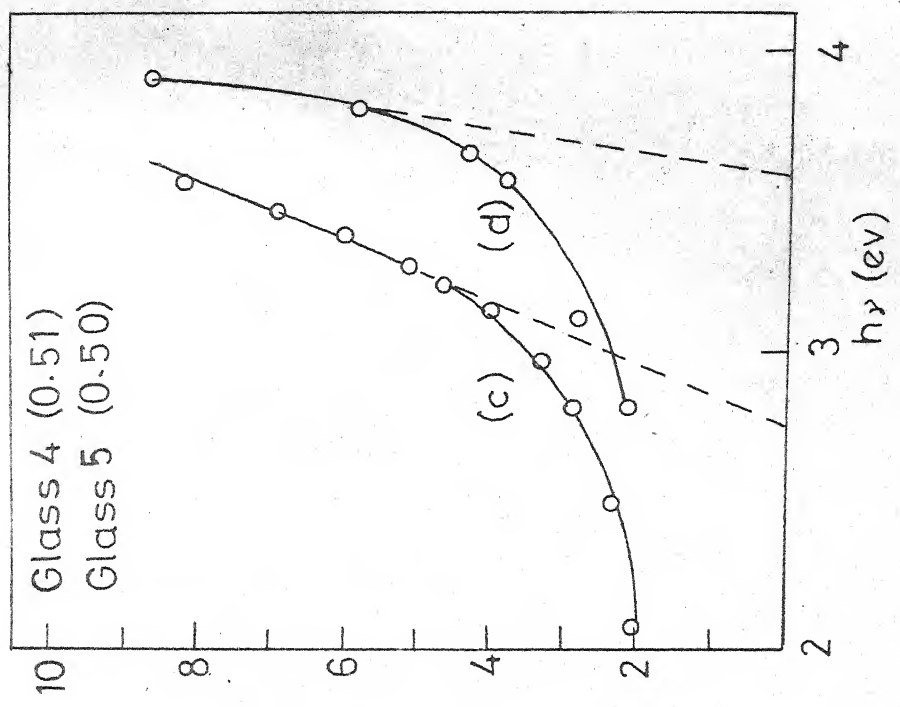


Fig. 25 Plot of  $\sqrt{4h}$  vs.  $h^*$  for different glasses (Numbers in bracket indicate thickness of specimen in mm)

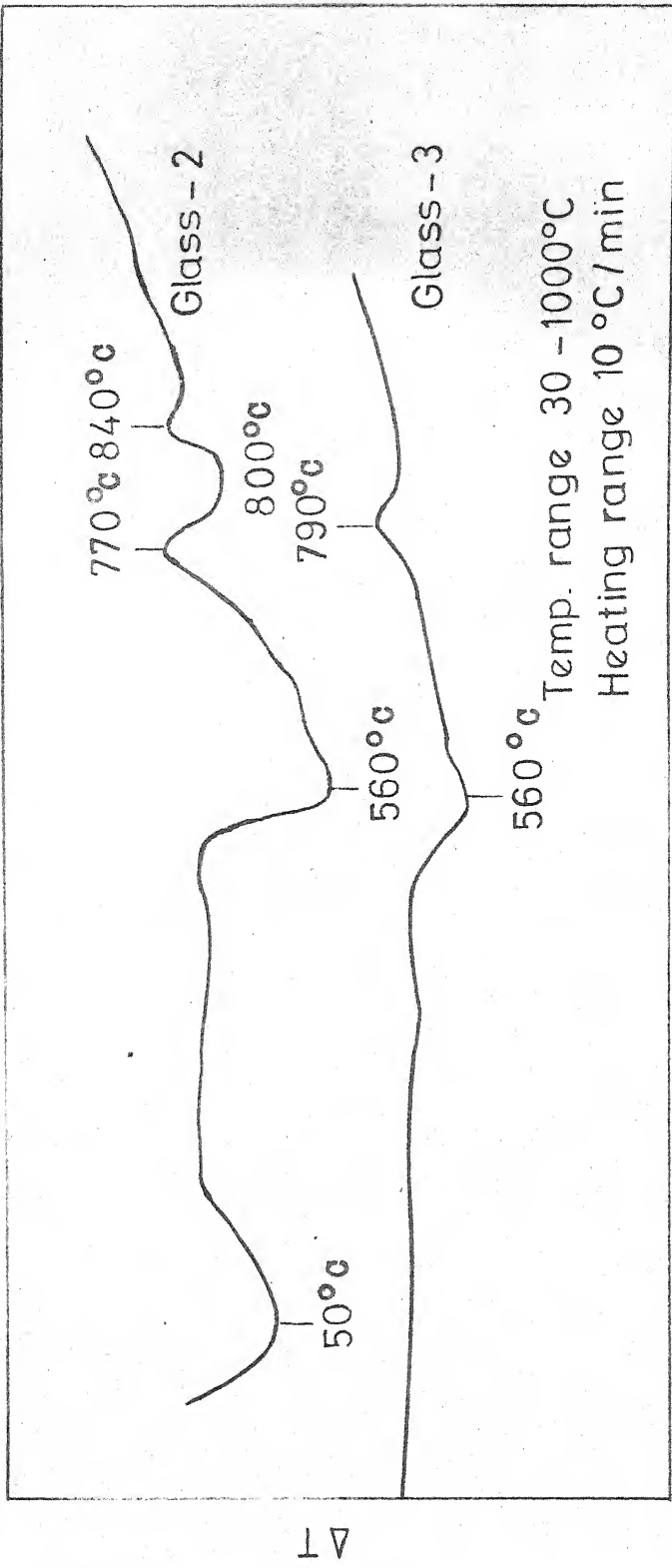


Fig. 26 DTA curves for virgin glasses 2 and 3

CHAPTER VDISCUSSION5.1 Bulk Resistivity

For bulk resistivity, the  $\log \frac{1}{\rho}$  vs  $1/T$  plots show two distinct activation energies. The variation of resistivity with temperature and activation energy values which are about 1 eV, for the glasses indicate that the conductivity would arise due to movement of alkali ions. For glasses 1, 2, 4, 5 and 12 there is deviation from linearity at high temperatures. This could be due to polarisation at the electrodes. The charges collect at the electrodes and resist the flow of charge carriers which is responsible for high resistance. The fact that glass 23 which contains less mole % of  $\text{Na}_2\text{O}$  does not show polarisation may support the fact the conduction in these glasses is due to sodium ions. However, it is to be noted that for all the glasses the linearity of I-V plots was maintained. This casts some doubt on the above explanation of polarisation effect. In order to confirm the effect of polarisation, one should carry out a.c. measurements for these glasses.

In Fig. 10, the variation of activation energy with the ratio of concentration of  $\text{Sb}_2\text{O}_3$  to  $\text{Bi}_2\text{O}_3$  is

shown. We observe a peak in activation energy when the ratio  $Sb_2O_3/Bi_2O_3$  is about one. This may be explained as follows. In the borosilicate glasses containing both  $Sb_2O_3$  and  $Bi_2O_3$ , bismuth can be considered to act as network modifier, and antimony can be considered to act both as network former as well as network modifier.<sup>(67)</sup> It may be possible that as the ratio of  $Sb_2O_3/Bi_2O_3$  increases first  $Sb^{3+}$  ions occupy the "network forming" sites and the network becomes more and more rigid. The activation energy would thus increase. When the ratio  $Sb_2O_3/Bi_2O_3$  becomes unity,  $Sb^{3+}$  ions may start acting as network modifier like  $Bi^{3+}$  ions. The network becomes less and less rigid, lowering the activation energy.

For the temperature range 225 to 310°C in the plot of activation energy vs. the ratio of  $Sb_2O_3/Bi_2O_3$  (Fig. 11) there is no peak in the activation energy. At the high temperature  $Sb^{3+}$  ions may not act as network former but may act as network modifier, which accounts for lowering of the activation energy as  $Sb_2O_3/Bi_2O_3$  increases. The activation energy is lower at high temperature which is characteristic of ionic conduction. However, this explanation might have to be reviewed seriously if electrode polarization effect is proved to be dominant in this temperature range.

In some of the glasses cooling curves show linear behaviour and differ from heating curves. This could be attributed to the effect of heat treatment given to the sample during heating cycle.

## 5.2 Surface Resistivity

Borosilicate glasses containing  $\text{As}_2\text{O}_3$  and  $\text{Sb}_2\text{O}_3$  have shown peculiar behaviour in the variation of surface resistivity with temperature<sup>(59,63)</sup>. It has been observed that in these glasses, as the temperature is increased from room temperature the resistivity increases (which is contradictory to usual behaviour) upto certain temperature and then it decreases. Whereas, when the temperature is decreased from room temperature, there was a sudden increase of resistivity. Thus the resistivity has a dip at the room temperature. This has been explained as follows.

It has been assumed that, water molecules adsorbed on the surface do play a role in determining the surface resistivity. The increase of resistivity with temperature has been explained due to protons acting as charge carriers. Protons are thought to be present in hydroxyl group and these migrate to near by terminal oxygen atoms under the action of an electrical field<sup>(65)</sup>. Conductivity increases

with the concentration of both the OH groups and the terminal oxygen atoms. Since the sum of these concentrations is constant, there is an optimum ratio of concentration at which conductivity is greatest.

As the temperature of sample is increased from room temperature, some of water molecules may be driven off and hence the surface resistivity is increased. Above a certain temperature, the decrease in surface resistivity has been explained as of alkali ions. As the temperature is lowered below room temperature the sudden increase of resistivity has been explained due to the upsetting of the optimum ratio between the concentration of OH groups and terminal atoms, as the water content is increased.

Since our glasses under investigation have similar glass matrix as in the case of  $\text{As}_2\text{O}_3$  or  $\text{Sb}_2\text{O}_3$ , one would expect the similar behaviour for our glass also. We shall discuss this in detail in next sections.

#### 5.2.1 Virgin glasses

For glasses 1, 3, 4 and 5 (with 10 mole %  $\text{Na}_2\text{O}$ ) the plots of  $\log \frac{\sigma}{T}$  vs.  $1/T$  are as shown in figure 11. The plots are all linear and the activation energies are of the order of 1 eV. Glasses 11, 12 and 13 (with 5, 3, 1 mole %  $\text{Na}_2\text{O}$  respectively) show a peak in the resistivity

The orders of the magnitudes of surface resistivities of the reduced glasses 2, 3, 11 and 12 (Figs. 13 and 14) are much less than that of the virgin glasses (Figs. 11 and 12). This may be attributed due to presence of conducting islands of bismuth and antimony as shown from microstructural studies. The activation energies for reduced glasses are of the order 0.3 eV compared to 1 eV for virgin glasses. One possibility for lowering of the activation energy is that it arises from electron hopping between two conducting islands, as the conduction mechanism in the reduced glasses.

For glass 13 (Fig. 15), the order of magnitude of surface resistivity is comparable to that of virgin glasses. This can be explained as for the glass 13 reduction may not be complete. Perhaps, low concentration of  $\text{Na}_2\text{O}$  may cause partial reduction.

### 5.2.3 Ion-exchanged and reduced glasses

#### 5.2.3.1 Low temperature measurements

In the low temperature regions of the plots  $\log \sigma$  vs.  $1/T$ , for IER glasses (figures 17 to 20) we see that the activation energies are low as given in Table 2. The low activation energy observed in low temperature

re ion for the glasses can be attributed to electron hopping between conducting islands as explained below.

As discussed in Chapter I, the microstructure of ion-exchanged and reduced glasses containing  $\text{Bi}_2\text{O}_3$  and  $\text{Sb}_2\text{O}_3$  separately has been shown to consist of a dispersion of particles of antimony, bismuth and silver. These are considered to act like conducting islands. The diameter of these conducting islands of bismuth can be approximately calculated using Neugebauer and Webb model<sup>(64)</sup>. The activation energy ( $\phi$ ) as given by the model is

$$\phi = \frac{e^2}{K r}$$

where  $e$  = charge of electron;  $K$  = dielectric constant of glass matrix, and  $r$  = size of conducting islands. Assuming a value of  $K = 6$  and  $\phi = 0.08$  eV for our glass system, we get  $r = 45 \text{ \AA}$ . This is consistent with the microstructural features of the glasses.

### 5.2.3.2 High temperature measurements

The plots of  $\log \beta$  vs.  $1/T$  for ion-exchanged and reduced glasses show peculiar behaviour. By comparing the plots of  $\log \beta$  vs.  $1/T$  for IER glasses and virgin glasses we find in the temperature range

about 50-120 $\Omega$ . The orders of magnitudes of surface resistivities of IER glasses are less than that of the virgin glasses. As in the case of reduced glasses, this can also be attributed to the presence of conducting islands.

To observe peaks and dips in the plots for glass 2, 3, 4, 5 and 21 as shown in figures (17-20 and 23). By examining the plots we see that as the ratio of concentration of  $Sb_2O_3$  to  $Bi_2O_3$  decreases

- (i) The peaks and dips disappear gradually (there is no peak for glass 1 where the ratio  $Sb_2O_3/Bi_2O_3$  is 0.2 as shown in Fig. 16).
- (ii) Temperature at which the minimum resistivity occurs, shifts towards higher temperature (for glasses 5, 4, 3, 2 and 21 the temperature shifts from room temperature to 70°C).

In borosilicate glasses containing  $As_2O_3$  and  $Bi_2O_3$  separately, similar peculiarities with temperature have been observed. But for those glasses minima of resistivity have been found to occur always at room temperature. This behaviour has been explained as the effect of adsorption of water by the glass surfaces as described earlier.

about 50-320°C. The orders of magnitudes of surface resistivities of IER glasses are less than that of the virgin glasses. As in the case of reduced glasses, this can also be attributed to the presence of conducting islands.

We observe peaks and dips in the plots for glass 2, 3, 4, 5 and 21 as shown in figures 17-20 and 23. By comparing the plots we see that as the ratio of concentration of  $Sb_2O_3$  to  $Bi_2O_3$  decreases

- (i) The peaks and dips disappear gradually (there is no peak for glass 1 where the ratio  $Sb_2O_3/Bi_2O_3$  is 0.2 as shown in Fig. 16).
- (ii) Temperature at which the minimum resistivity occurs, shifts towards higher temperature (for glasses 5, 4, 3, 2 and 21 the temperature shifts from room temperature to 70°C).

In borosilicate glasses containing  $As_2O_3$  and  $Sb_2O_3$  separately, similar peculiarities with temperature have been observed. But for those glasses minima of resistivity have been found to occur always at room temperature. This behaviour has been explained as the effect of adsorption of water by the glass surfaces as described earlier.

However, the above explanation may not hold good in explaining the nature of variation of  $\log \varphi$  with  $1/T$  for glasses containing both  $Sb_2O_3$  and  $Bi_2O_3$  since the temperature at which the minimum of resistivity occurs, shifts towards the high temperature. Perhaps, the water adsorption may not play a role in conduction process for our glass systems.

As we know there will be drastic changes in the physical properties of materials undergoing structural transitions. One can also expect that some sort of structural transition may be occurring in our glass systems. The dips and peaks of the plots of  $\log \varphi$  vs.  $1/T$  may then be considered to arise from some structural transition which may be taking place in these glasses at the particular temperature.

However, the above observed nature of the variation of resistivity with temperature for our glass systems may be due to the combined effect of antimony, bismuth and silver particles as these are shown to be present in ion-exchanged and reduced glasses.

In order to confirm whether the behaviour is due to water adsorption or not one should carry out the measurements in vacuum or by passing dry nitrogen over the sample.

### 5.3 Switching

IER glasses 1, 2 and 4 have been found to show "memory type" switching. As explained in Chapter 1, the switching in the IER glasses containing  $\text{Bi}_2\text{O}_3$  could probably arise due to a crystallisation process induced in the glass phase between the metallic particles. The same process may also be thought of to be effective in the glasses under investigation. Further studies have to be done on glasses containing both  $\text{Sb}_2\text{O}_3$  and  $\text{Bi}_2\text{O}_3$  in order to find the combined effect of these oxides.

### 5.4 Optical Absorption

For virgin glasses 2, 3, 4 and 5, the absorption edge was observed at about  $3000 \text{ \AA}^{\circ}$ . The absorption edges lie in the range of 2.7 to 3.7 eV. As we see, these are more than twice the activation energy determined by d.c. measurements for these glasses. This is consistent with the results of other oxide glasses<sup>(23)</sup>.

### 5.5 Differential Thermal Analysis

DTA curves for glasses 2 and 3 show an endothermic peak at about  $560^{\circ}\text{C}$  and exothermic peak at about  $790^{\circ}\text{C}$ . The endothermic peak may be thought of as arising due to

crystallisation. However when heat treatment was given to glass 2, no crystallisation was observed. This would cast doubt on the above explanation. An endothermic peak at about 50°C for glass 2 may be due to expelling of water molecules adsorbed in the glasses.

## CHAPTER 6

### CONCLUSION AND SCOPE FOR FURTHER WORK

#### 6.1 Conclusions

From the experimental studies, made on the borosilicate glasses containing both  $Sb_2O_3$  and  $Bi_2O_3$ , the following conclusions could be drawn.

- (i) The rigidity of borosilicate glass matrix depends on the ratio of concentration of  $Sb_2O_3$  to  $Bi_2O_3$  and the network coherence seems to be maximum when the ratio is one.
- (ii) The d.c. electrical conductivity of these glasses in the temperature range 50–400°C is due to the motion of alkali ions.
- (iii) The orders of magnitudes of surface resistivities of the reduced and the ion-exchanged and reduced glasses are less than that of virgin glasses and this is attributed to the presence of conducting islands of either antimony or bismuth or silver or a combination of these three.
- (iv) The surface resistivities of ion-exchanged and reduced glasses show dips and peaks in the plots of  $\log \rho$  vs.  $1/T$ . The minima of the surface

resistivity move toward high temperature as the ratio of the concentration of  $Sb_2O_3$  to  $Bi_2O_3$  decreases.

This behaviour cannot be attributed to the effect of water adsorption and may be considered to arise from some structural transitions occurring in these glasses at these temperatures.

- (v) Conduction in the ion-exchanged and reduced glasses at low temperatures arises due to the electron hopping between the conducting islands. This is consistent with the microstructural features of the glasses.

## 6.2 Scope for Further Studies

- (i) To study in detail the microstructure of the glasses and to characterise the different phases before and after the surface treatments (like ion-exchange or reduction) given to them.
- (ii) The variations of surface resistivities of the glasses containing  $Bi_2O_3$ - $Sb_2O_3$ ,  $As_2O_3$  and  $Sb_2O_3$  with temperature have showed peculiar behaviour. It will be interesting to study the variation of surface resistivities of borosoda glasses containing combinations of above ingredients like  $As_2O_3$ - $Bi_2O_3$ ,  $Sb_2O_3$ - $As_2O_3$ .

(iii) In order to study the effect of water adsorption of the glasses, it is necessary to carry out the measurements in vacuum or in an inert atmosphere.

REFERENCES

1. R.G. Neale, J. Non-cryst. Solid, 2 (1970) 558.
2. D. Pai and S.W. Ing, Phy. Rev., 173 (1968) 729.
3. E.P. Denton, H. Rawson and J.E. Stanworth, Nature, London, 173 (1954) 10.
4. J.D. Mackenzie, "Semiconducting Oxide Glasses" in Modern Aspects of the Vitreous State, ed. J.D. Mackenzie, Vol. 3 (1964), Butterworths (Washington).
5. J.D. Mackenzie, J. Am. Ceram. Soc., 47 (1964) 211.
6. R. Tsu et.al., J. Non-cryst. Solids, 4 (1970) 322.
7. A.M. Andreiash and B.T. Kolomietz, Soviet Phys. Solid State, 6 (1965) 2652.
8. M.H. Bcdsky et.al., Phys. Rev. B1, (1970) 2632.
9. H.L. Uphoff and J.H. Healy, J. Appl. Phys., 32 (1961) 950.
10. J.T. Edmond, J. Non-cryst. Solids, 1 (1958) 39.
11. H. Fritzsche, 'Electronic & Structural Properties of Amorphous Semiconductors.'
12. R. Collerbs, M. Denayer, F.H. Hashmi and G.D. Petit, Discussions of Faraday Soc., 50 (1970) 27.
13. L. Banyai, Physique des semiconductors (Dunod, Paris, 1960) 147.

14. N.F. Mott, *Advan. Phys.*, 16 (1967) 49.
15. E.A. Fagen and H. Fritzsché, *J. Non-cryst. Solids*, 2 (1970) 170, 180.
16. M. Pollak & T.H. Geballe, *Phy. Rev.*, 122 (1961) 1742;  
M. Pollak, *Phys. Rev.*, 133 (1964) A564.
17. A.E. Owen and J.M. Robertson, *J. Non-cryst. Solids*, 2 (1970) 40.
18. H.P.D. Lanyon, *Phys. Rev.*, 130 (1961) 134.
19. J.L. Hartke, *Phys. Rev.*, 125 (1962) 1177.
20. B.T. Kolomietes and E.A. Lebedev, *Soviet Phy. Semiconductors*, 1 (1967) 244.
21. R.S. Allgaier, in: *Proc. 9th Intern. Conf. on the Physics of Semiconductors*, Moscow, (1968).
22. M.D. Tabak and P.J. Warter, *Phys. Rev.*, 173 (1968) 729.
23. Y. Toyozawa, *Tech. Report of the Inst. for Solid State Physics* (Univ. of Tokyo) Ser. A No. 119 (1964).
24. H.P.D. Lanyon, *Phys. Rev.*, 125 (1962) 1177.
25. J. Tauc, in: *Optical Properties of Solids*, Ed. F. Abeles (North Holland, Amsterdam, 1969).
26. T.M. Donovan, and W.E. Spicer, *Phys. Rev. Letters*, 21 (1968) 1572.
27. J.T. Littleton and G.W. Morey, *The Electrical Properties of Glass*, Wiley, New York, 1953.

28. E. Rasch and F. Hinrichsen, *Z. Electrochem.*, 14 (1908) 41.
29. J. Frenkel, *Kinetic Theory of Liquids*, Oxford Univ. Press, London, (1946).
30. J.M. Stevcls, *Encyclopedia of Physics*, Vol. 20, 350, Springer-Vorlag, Berlin (1957).
31. O.V. Mazurin, *Electrical Properties and Structures of Glass*, Consultants Bureau, New York (1965).
32. R.H. Doremus, in: *Modern Aspects of the Vitreous State*, Vol. 2, Chap. 1, Butterwcrths, Washington D.C. (1962).
33. R.H. Doremus, *J. Phys. Chem.*, 68 (1964) 2212.
34. B. Lenggel and Z. Boksař, *Z. Phys. Chem.*, 203 (1954) 93; 204 (1955) 157.
35. J.O. Isard, *J. Non-cryst. Solids*, 1 (1969) 235.
36. J.R. Johnson, R.H. Bristow and H.H. Blau, *J. Am. Ceram. Soc.*, 34 (1965) 135.
37. R.J. Charles, *J. Am. Ceram. Soc.*, 45 (1962) 105.
38. J.T. Littleton and W.L. Wetmore, *J. Amer. Ceram. Soc.*, 10 (1936) 243.
39. M.H. Cohen, H. Fritzsche and S.R. Ovshinsky, *Phys. Rev. Letters*, 22 (1969) 1065.
40. N.F. Mott, *Advan. Phys.*, 16 (1967) 49.
41. N.F. Mott, *Phil. Mag.*, 22 (1970) 7.
42. N.F. Mott and E... Davis, *Electronic Processes in Non-crystalline Materials*, Clarendon Press, Oxford, 1971.

43. P.W. Anderson, Phys. Rev., 109 (1958) 1492.
44. A.I. Gubanov, Quantum Theory of Amorphous Conductors, Consultants Bureau, New York, 1965.
45. K. Hulls and P.W. Mcmillan, J. Phys. D. Appl. Phys., 5 (1972) 67.
46. A.D. Pearson, J. Non-cryst. Solids, 2 (1970) 1.
47. H.R. Fritzsche, J. Non-cryst. Solids, 2 (1970) 393.
48. K.V. Roer and S R. Ovshinsky, J. Appl. Phys., 41 (1970) 2675.
49. A.D. Pearson, IBM J. Res. Develop., 13 (1969) 510.
50. S.R. Ovshinsky, J. Non-cryst. Solids, 2 (1970) 99.
51. J.J. O'Dwyer, J. Electrochem. Soc., 116 (1969) 239.
52. D. Eaton, J. Am. Ceram. Soc., 47 (1964) 554.
53. R.L. Green and K.B. Blodgett, J. Am. Ceram. Soc., 31 (1948) 89. (1970) 510
54. K.B. Blodgett, J. Am. Ceram. Soc., 34 (1951) 14.
55. A.K. Varshneya, J. Non-cryst. Solids, 19 (1975) 355.
56. D. Chakravorty, J. Non-cryst. Solids, 15 (1974) 191.
57. D. Chakravorty, A. Shuttleworth and P.H. Gaskell, J. Materials Science, 10 (1975) 799.
58. D. Chakravorty, Appl. Phys. Letters, 24 (1974) 62.
59. Devendra Kumar . M.Tech. Thesis, I.I.T. Kanpur (1975).
60. D. Chakravorty and C.S. Murthy, J. Phys. D. Appl. Phys., 8 (1975) 2162.

61. D. Chakravorty, to be published.
62. W.H. Omar, M. El. Hamamsy and A. Bishay, Proc. 9th Int. Congr. on Glass, Versailles (1971) 521.
63. Halliyal Arvind, M.Tech. Thesis, I.I.T. Kanpur (1976).
64. C.A. Neugebauer and M.B. Webb, J. Appl. Phys., 33 (1962) 74.
65. S. Lizima, M. Surgi, N. Kikuchi and K. Tanaka, Solid State Communications, 9 (1971) 795.
66. J. Fauc et.al., in Physics of Non-crystalline Solids, Ed. J.A. Prins, North Holland, Amsterdam (1965) 606.
67. J. Stanworth, Physical Properties of Glasses, Oxford, Clarendon Press (1953).